REPORT DOCUMENTATION PAGE

Form Approved OMB No. 0704-0188

1. REPORT DATE *(DD-MM-YYYY)*	2. REPORT TYPE	3. DATES COVERED *(From – To)*
10-09-2002	Final Report	17 July 2001 – 17 July 2002

4. TITLE AND SUBTITLE

Effects Of Averaging Mass On Predicted Specific Absorption Rate (SAR) Values

5a. CONTRACT NUMBER
F61775-01-WE041

5b. GRANT NUMBER

5c. PROGRAM ELEMENT NUMBER

6. AUTHOR(S)

Dr. Peter Gajsek

5d. PROJECT NUMBER

5d. TASK NUMBER

5e. WORK UNIT NUMBER

7. PERFORMING ORGANIZATION NAME(S) AND ADDRESS(ES)

National Institute of Public Health
Trubarjeva 2
Ljubljana 1000
Slovenia

8. PERFORMING ORGANIZATION REPORT NUMBER

N/A

9. SPONSORING/MONITORING AGENCY NAME(S) AND ADDRESS(ES)

EOARD
PSC 802 BOX 14
FPO 09499-0014

10. SPONSOR/MONITOR'S ACRONYM(S)

11. SPONSOR/MONITOR'S REPORT NUMBER(S)
SPC 01-4041

12. DISTRIBUTION/AVAILABILITY STATEMENT

Approved for public release; distribution is unlimited.

13. SUPPLEMENTARY NOTES

14. ABSTRACT

This report results from a contract tasking National Institute of Public Health as follows: The contractor will investigate the role of averaging mass on calculated specific absorption rate (SAR) values in predicting the effects of radiofrequency radiation (RFR) exposures on body tissues and organs. A Finite Difference Time Domain (FDTD) program will be used to predict localized and whole body SAR values in 3-dimensional anatomical model of a human. Results will address the error margin in RF dosimetry.

15. SUBJECT TERMS
EOARD, Biology, Mathematical Modeling, Radiofrequency Radiation, Bioeffects

16. SECURITY CLASSIFICATION OF:			17. LIMITATION OF ABSTRACT	18, NUMBER OF PAGES	19a. NAME OF RESPONSIBLE PERSON
a. REPORT	b. ABSTRACT	c. THIS PAGE			Valerie Martindale, Maj, USAF
UNCLAS	UNCLAS	UNCLAS	UL	48	**19b. TELEPHONE NUMBER** *(Include area code)* +44 (0)20 7514 4437

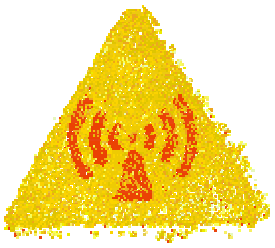

Dr. Peter Gajšek
Pohorskega bat. 215a
1000 Ljubljana, SLOVENIA
☎ +386 1 568 2732,
e-mail:peter.gajsek@3rtim.si

RESEARCH PROJECT:

Contract agreement No.: F61775-01W-E041

EFFECTS OF AVERAGING MASS ON PREDICTED SPECIFIC ABSORPTION RATE (SAR) VALUES

FINAL REPORT

SEPTEMBER 2002

Ljubljana, SLOVENIA

(1) In accordance with Defense Federal Acquisition Regulation 252.227-7036, Declaration of Technical Data Conformity (Jan 1997), All technical data delivered under this contract shall be accompanied by the following written declaration:

"The Contractor, Dr. Peter Gajšek, hereby delcares that, to the best of his knowledge and belief, the technical data delivered herewith under Contract No. F61775-01-WE041 is complete, accurate, and complies with all requirements of the contract.

DATE: July-17-2002
Name and Title of Authorized Official: Dr. Peter Gajšek

(2) In accordance with the requirements in Federal Aquisition Regulation 52.227-13, Patent Rights—Acquisition by the U.S. Government (Jun 1989), CONTRACTOR WILL INCLUDE IN THE FINAL REPORT ONE OF THE FOLLOWING STATEMENTS:

(B) "I certify that there were no subject inventions to declare as defined in FAR 52.227-13, during the performance of this contract."

DATE: July-17-2002
Name and Title of Authorized Official: Dr. Peter Gajšek

ACKNOWLEDGMENT:
This material is based upon work supported by the European Office of Aerospace Research and Development, Air Force Office of Scientific Research, Air Force Research Laboratory, under Contract No. F61775-01-WE041.

DISCLAIMER:
Any opinions, findings and conclusions or recommendations expressed in this material are those of the author(s) and do not necessarily reflect the views of the European Office of Aerospace Research and Development, Air Force Office of Scientific Research, Air Force Research Laboratory.

1. INTRODUCTION

Millimeter resolution of the experimental measurements and anatomically-based numerical models of the head and torso of humans has, in some cases, led to questions of interpretation of the appropriate volume over which spatial peak specific absorption rate (SAR) values should be averaged.

The standards for human protection against electromagnetic fields (EMF) in the radio frequency (RF) range are primarily based on the concept of a thermal mechanism and protect only against "thermal" effects. Indeed, the current consensus is that only thermal RF effects could be harmful, but this certainly does not mean that studies reporting possible non-thermal effects were ignored. This consensus is based on rigorous analysis of published studies, which have to satisfy such strict criteria as replication in several species, under different field conditions, and that the effects could be considered potentially harmful in humans. A brief review of some RF safety standards, such as the International Commission of Non-ionizing Radiation Protection (ICNIRP) and Institute of Electrical and Electronics Engineers, Inc. (IEEE) standards [ICNIRP 1998, IEEE 1999], reveals that they now include consideration of frequency dependent absorption in human body (whole body resonance). In addition, special restrictions on localized exposure including methods for volume averaging are introduced. These documents specify time-averaged whole-body-averaged SARs and peak spatial-average SARs, neither of which should be exceeded. The spatial peak SAR is usually averaged over a specified volume, e.g., 1 gram of tissue in the shape of a cube [IEEE 1999] or 10 grams of contiguous tissue [ICNIRP 1998].

Current RF exposure standards are generally derived from an assumption of uniform field exposure of the entire body. While the fundamental basis of these standards is related to limiting the SAR in the body, as averaged over the entire body mass, most standards, such as those of the IEEE [1999] and ICNIRP [1998], also contain Maximum Permissible Exposure (MPE) limits and reference levels related to peak SAR that may occur at any point within the body, usually averaged over either 1 or 10 grams of tissue. These spatial peak SAR limits are derived from observations of uniform exposure of laboratory animals and phantom models of both animals and humans. In recognition of the non-uniform absorption of RF energy within the body, even with uniform field exposure over the body, the standards set a limit on the spatial peak SAR at 20 times the whole-body average value. For example, while the whole-body average SAR is limited to 0.4 watts per kilogram (W/kg) in the whole body, a local SAR of 8 W/kg, averaged over 1 gram of tissue, is permitted.

Further complicating this issue is the fact that the FDTD voxel size is not always (in fact, it rarely is) divisible into exactly 1 g or 10 g cubes. While it is possible to use interpolation or extrapolation of data to reduce the problem, the difficulties of handling surface structure and heterogeneous tissue masses remain. Since the fields from near-field sources decay rapidly away from the source, the size of the volume and the percentage of tissue encompassed can have a significant effect on the results.

The objective of this study is to investigate the role of averaging mass on maximal localized SAR and, therefore, to identify the most sensitive and critical survival organs where the highest localized SAR versus whole body SAR values are reported. This work contributes to understanding the role of various technical approaches in relation to calculate the spatial peak SAR averaged over certain mass of tissue. This satisfies the requirement to quantify the SAR dependence on various model parameters and leads to increased confidence in the validity of the numerical calculations. In addition, it investigates also the error margin in RF dosimetry.

2. DESCRIPTION OF THE PROJECT

This research project focuses on the role of the averaging mass interval (1g, 10g) on spatial peak SAR values in various resolutions of the anatomical man model and exposure conditions with special emphasis on maximal absorption in critical survival organs. To identify the spatial peak SAR value in each individual tissue/organ averaged over certain mass intervals, various techniques for altered exposure conditions (frequency, orientation) were investigated. Inter-comparison of the data represents a basis for setting a criteria for more accurate numerical dosimetry. Further, spatial peak SAR in critical tissues/organs averaged over various masses was compared to average whole body SAR. High SAR values in tissue near a blood vessel may be less consequential than a high SAR deep in muscle, whereas high SAR in muscle tissue may be less consequential than high SAR in lung tissue [Chou et al. 1996] . Thus, localized SAR in the brain and spinal cord seem to be more appropriate parameter for risk assessment than the whole body SAR value. This work provides important information on the critical organ absorption in relation to various exposure conditions. Since exposure conditions play an important role in absorption of electromagnetic energy in biological systems, detailed analysis of the maximum absorption in relation to the frequency and orientation for each target tissue/organ was completed.

One of the goals of this study is also to develop a numerical technique for the computation of localized SAR averaged over certain mass interval. Since various approaches towards the averaging procedures are reported, their inter-comparison will provide a detailed insight into the advantages and disadvantages of each used method. Various averaging techniques were used in identification of the target tissues and organs where the highest ratios between spatial peak SAR and averaged whole body SAR occur.

This final report covers activities as follows:

Phase 1: Construction of the modified resolution of the digital anatomical model of the man (3, 10, and 22 mm^3 voxel size),

Phase 2: Inter-comparison of the whole body and spatial peak SAR for various voxel sizes of the models

Phase 3: Inter-comparison of different algorithm for computations of power deposition in different volume (1g and 10 g) of the tissue

Phase 4: Analysis of the spatial peak SAR values in critical survival organs in 3 mm^3 man model by using various algorithms.

3. METHODOLOGY – VARIOUS RESOLUTIONS OF THE HUMAN DIGITAL ANATOMICAL MODEL

The Finite Difference Time Domain (FDTD) program based on code originally described by Kunz and Luebbers [1993] was used to predict localized and whole body SAR values in 3-dimensional anatomical model of a man. The FDTD code and digital anatomical models were developed jointly by U.S. Naval Health Research Center Detachment and U.S. Air Force Research Laboratory, Brooks AFB, Texas. The permittivity properties of each of the tissue types are set according to data and fits published by Gabriel [1996]. The code reads the anatomical model files obtained from Visible man and outputs a number of files which include 3-D normalized SAR; mean, minimum, and maximum SARs for each tissue type; and each Z-plane slice. In addition, a special software program was developed to perform the averaging of the output SAR file over desired mass. The human model is based on the photographic data from Visible Human Project created by the National Library of Medicine (http://www.nlm.nih.gov/research/visible/visible_human.html) and the University of Colorado Health Science Center (http://www.uchsc.edu/sm/chs/).

A computer-segmented set of the photographic images was created by the National University of Singapore and Johns Hopkins University. We limited the number of tissue types based on their size in the body and availability of permittivity properties. Each of 1878 slices in the XY plane was coded by hand using Adobe Photoshop ™ and a palette of colors that represented 40 tissue types (See Mason et al. [1995, 1999] for a complete description). It is the largest of the anatomical data sets we have created at 374 million voxels (1878 by 340 by 586). Each voxel is a cube 1 mm on a side. Modeling EMF exposures with this model will require approximately 18 GB of computer memory for finite-difference time-domain (FDTD). Since high

resolution model requires lots of computer memory, smaller versions of this data set have been created and are suitable for some applications with considerably less memory required.

The initial anatomical data sets contained 374 million voxels (1878 by 340 by 586) with each voxel being a cube 1 mm on a side. Calculating EMF exposures with this model requires approximately 18 GB of computer memory for FDTD. Because of the limited power of available computers, we therefore used a smaller version of this data set with a resolution of 3 mm^3 (626 by 114 by 196 voxels). In addition, existing voxel size of the man is changed in such a way that mass of the voxel corresponds to the standardized averaging mass interval (1 g requires voxel size of 10 mm^3 (188 by 34 by 59 voxels), 10 g requires voxel size of 22 mm^3 (86 by 16 by 27 voxels)). These modified digital models are used as an input to FDTD code.

These reduced resolution models are created automatically. The process would be as follows for creating a 3-mm anatomical model from a 1-mm model. Layers of air are added to one or more sides of the model volume to make the size of the model an even multiple of the 3 mm^3. The reduction would then take a cube of 3 by 3 by 3 one-millimeter voxels and based on the most common type in that cube create a single three-millimeter voxel. This process would be repeated for each 3 by 3 by 3 set of 1-mm voxels. The same process is used for creating 10 and 22 mm cubic voxels.

Figure 1. Digital anatomical model of the human developed by Brooks AFRL

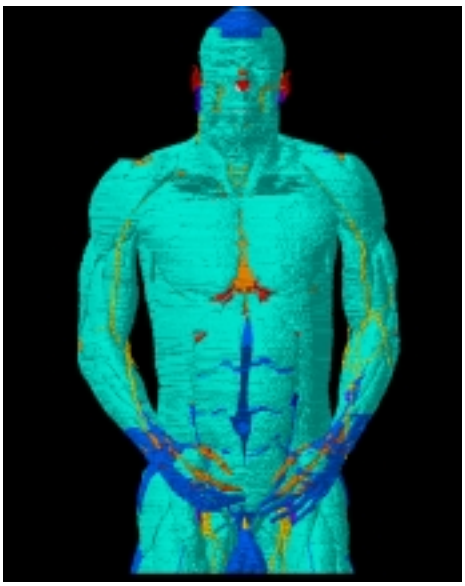

The choice of cell size of the applied anatomical man model is critical in applying FDTD. It must be small enough to provide accurate results at the highest frequency of interest, and yet be large enough to keep resource requirements manageable. Cell size is directly affected by the dielectric properties of the materials present. The greater the permittivity and/or conductivity the shorter the wavelength at a given frequency and the smaller the cell size required. Once the cell size is selected, the maximum time step is determined by the

Courant stability condition. After the cell size is determined, the problem space large enough to encompass the scattering object, plus the space between the object and the outer absorbing boundary, are defined. From the number of Yee cells needed and the number of time steps required, resource requirements can be estimated [Kunz and Luebbers 1993]. The fundamental constraint is that the cell size must be much less than the smallest wavelength, for which accurate results are required. An often quoted constraint is "10 voxels per wavelength," meaning that the side of each cell should be 1/10 of the wavelength at the highest frequency (shortest wavelength) of interest. Since FDTD is a volumetric computational method, if some portion of the computational space is filled with penetrable material, one must use the wavelength in the material to determine the maximum voxel size. For problems containing biological materials this results in cells in the material that are much smaller than if only free space and perfect conductors were being considered.
Therefore,

$$voxel\ size \le 0.1\,\lambda = \frac{0.1\,c_0}{f\sqrt{\varepsilon_r}} \qquad \text{Equation 1.}$$

where
c_0 is the speed of light in vacuum (3×10^8 m/s),
f is frequency,
λ is wavelength, and
ε_r is relative dielectric constant of biological tissues.

The number of tissue types is based on their size in the body and availability of permittivity properties. In addition, increase in the voxel size introduces an error and, thus, very small organs may be distorted or lost, some symmetries may be affected, and the continuity of elongated structures may be disrupted (see Figure 2). The 3-mm^3 resolution man model consists of the 39 tissue-types, whereas 10 mm^3 model and 22 mm^3 model consist of 37 and 34 tissue types (see Table 1), respectively.

Figure 2. Sagittal views through the midline of the man model (for various voxel sizes) revealing normalized SAR values (W/kg/mW/cm^2) resulting from exposures in the EHK orientation to 70 MHz when the field was propagated in dorsal to ventral direction.

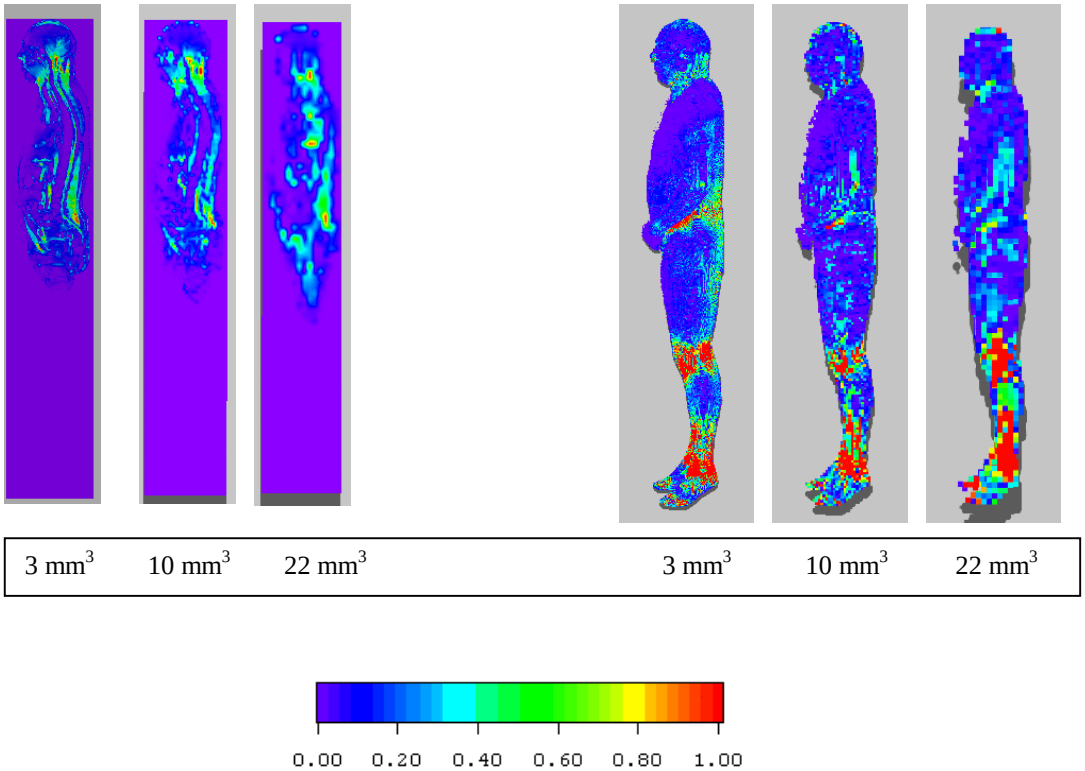

4. INTER-COMPARISON OF THE WHOLE BODY AVERAGED SAR FOR VARIOUS VOXEL SIZES OF THE ANATOMICAL MAN MODEL

The finite-difference time-domain program based on code originally described by Kunz and Leubbers [1993] is reported in numerous publications each year (www.fdtd.org) and has become one of the most frequently used methods to predict SAR values in organic and non-organic materials. The man model was processed at 3, 10, and 22 mm^3 resolution to determine the effects of voxel size on predicted SAR values, respectively.

Orientation of the object is defined by the incident-field vectors - E (electric field measured in V/m), H (magnetic field measured in A/m), and K (direction of propagation) - parallel to the long axis of the body. In our

study, we consider the dorsal (M) direction of propagation. Detailed description of various orientations is presented in Figure 3.

Figure 3. Representations of the three orientations examined (MEHK, MHEK, MKHE). The following three vectors comprise electromagnetic fields: the electric field (E-measured in V/m), magnetic field (H-measured in A/m), and direction of propagation (K). Orientation of the object with regard to the direction of propagation was dorsal (M).

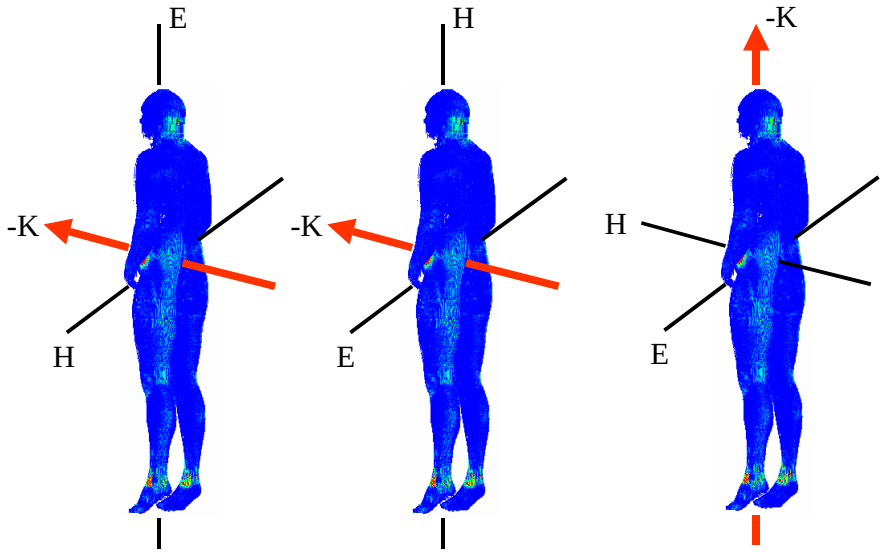

(MEHK) (MHEK) (MKEH)

The model was processed in the far field conditions at the resonant frequency (70 MHz) and non-resonant frequencies in the range between 35 - 2000 MHz for MEHK orientation. In addition, other orientations (MKEH, MHEK) of the model to the incident fields were used where no substantial resonant frequency exists.

The normalized whole body SAR (W/kg per mW/cm^2) values for the man (3 mm^3 voxel size) at a resonance frequency of 70 MHz are the highest in the MEHK orientation (0.27 W/kg per mW/cm^2), lower for MKEH (0.04 W/kg per mW/cm^2), and lowest for MHEK (0.02 W/kg per mW/cm^2). The normalized whole body SAR (W/kg per mW/cm^2) values for other voxel sizes (10 and 22 mm^3) showed pretty similar results. At a resonance frequency of 70 MHz the highest whole body SAR values are in the MEHK orientation (0.28 W/kg per mW/cm^2 for 10 mm^3 and 0.26 mW/cm^2 for 22 mm^3, respectively), lower for MKEH (0.03 W/kg per mW/cm^2 for 10 mm^3 and 0.025 mW/cm^2 for 22 mm^3, respectively), and lowest for MHEK (0.02 W/kg per mW/cm^2 for 10 mm^3 and

22 mm^3). These predicted whole-body SAR value are in good agreement with data published by Durney et al. [1986], Mason et al. [2000] and Gajsek et al. [2001].

Altering voxel size in the man model resulted in minor impact on the predicted normalized whole-body SAR values when the criterion (see Equation 1) was fulfilled. When the voxel size became greater than one-tenth of the wavelength the SAR values started to increase and could not be used for accurate prediction of the absorbed RF energy. When considering Equation 1 the voxel size of 22 mm^3 could be used up to 700 MHz and the model consisted of 10 mm^3 could be used up to 1100 MHz, respectively. This can be seen from Figures 5-7 where frequency dependent whole body SARs for various voxel sizes are presented.

Table 1. Identification number (ID), tissue types (Organ), their number of voxels (Voxel), mass of individual voxel in relation to its corresponding tissue (Voxel mass), and total Organ mass in the man model for various voxel sizes (3, 10, and 22 mm cubed).

		3 mm3			10 mm3			22 mm3		
ID	Organ	Voxel	Voxel Mass	Organ Mass	Voxel	Voxel Mass	Organ Mass	Voxel	Voxel Mass	Organ Mass
2	BILE	711	2.73E-05	1.94E-02	17	1.01E-03	1.72E-02	2	1.08E-02	2.15E-02
3	BODY FLUID	13575	2.73E-05	3.70E-01	369	1.01E-03	3.73E-01	37	1.08E-02	3.98E-01
4	EYE(cornea)	12	2.91E-05	3.49E-04	-	-	-	-	-	-
5	FAT	1245612	2.47E-05	3.08E+01	33742	9.16E-04	3.09E+01	3086	9.75E-03	3.01E+01
6	LYMPH	2677	2.81E-05	7.52E-02	67	1.04E-03	6.97E-02	12	1.11E-02	1.33E-01
7	MUSC. MEMBRANE	17621	2.81E-05	4.95E-01	486	1.04E-03	5.05E-01	45	1.11E-02	4.98E-01
8	NAILS (toe&finger)	128	2.78E-05	3.56E-03	6	1.03E-03	6.18E-03	-	-	-
11	NERVE (spine)	11764	2.80E-05	3.30E-01	329	1.04E-03	3.42E-01	29	1.11E-02	3.21E-01
17	MUSCLE	1588186	2.83E-05	4.49E+01	42888	1.05E-03	4.49E+01	4021	1.12E-02	4.48E+01
25	HEART	11320	2.78E-05	3.15E-01	305	1.03E-03	3.14E-01	22	1.10E-02	2.41E-01
30	WHITE MATTER	16348	2.80E-05	4.58E-01	456	1.04E-03	4.73E-01	40	1.11E-02	4.42E-01
48	STOMACH	5661	2.84E-05	1.61E-01	140	1.05E-03	1.47E-01	18	1.12E-02	2.01E-01
49	GLANDS	5705	2.84E-05	1.62E-01	158	1.05E-03	1.66E-01	12	1.12E-02	1.34E-01
65	BLOOD VESSEL	20845	2.81E-05	5.85E-01	568	1.04E-03	5.91E-01	52	1.11E-02	5.76E-01
68	LIVER	66244	2.78E-05	1.84E+00	1794	1.03E-03	1.85E+00	173	1.10E-02	1.90E+00
88	GALL. BLADDER	384	2.78E-05	1.07E-02	11	1.03E-03	1.13E-02	-	-	-
108	SPLEEN	8988	2.85E-05	2.56E-01	242	1.05E-03	2.55E-01	20	1.12E-02	2.25E-01
110	CEREBELLUM	4321	2.80E-05	1.21E-01	117	1.04E-03	1.21E-01	13	1.11E-02	1.44E-01
111	BONE (cortical)	92457	5.37E-05	4.97E+00	2481	1.99E-03	4.94E+00	244	2.12E-02	5.17E+00
133	CARTILAGE	18679	2.96E-05	5.53E-01	523	1.10E-03	5.74E-01	44	1.17E-02	5.14E-01
142	LIGAMENTS	93005	3.29E-05	3.06E+00	2538	1.22E-03	3.10E+00	265	1.30E-02	3.44E+00
143	SKIN/DERMIS	167810	3.04E-05	5.10E+00	4438	1.13E-03	4.99E+00	471	1.20E-02	5.64E+00
148	INTESTINE (large)	17155	2.82E-05	4.83E-01	462	1.04E-03	4.82E-01	45	1.11E-02	5.00E-01
152	TOOTH	489	5.83E-05	2.85E-02	7	2.16E-03	1.51E-02	1	2.30E-02	2.30E-02
160	GRAY MATTER	20628	2.80E-05	5.78E-01	564	1.04E-03	5.85E-01	48	1.11E-02	5.31E-01
163	EYE (lens)	22	2.84E-05	6.26E-04	-	-	-	-	-	-
164	LUNG (outer)	25849	2.84E-05	7.33E-01	701	1.05E-03	7.36E-01	53	1.12E-02	5.93E-01
168	INTESTINE (small)	28592	2.82E-05	8.05E-01	746	1.04E-03	7.78E-01	68	1.11E-02	7.55E-01
183	EYE (sclera/wall)	120	2.77E-05	3.32E-03	2	1.03E-03	2.05E-03	-	-	-
184	LUNG.(inner)	99832	7.02E-06	7.01E-01	2669	2.60E-04	6.94E-01	262	2.77E-03	7.25E-01
188	PANCREAS	3116	2.82E-05	8.79E-02	87	1.05E-03	9.09E-02	8	1.11E-02	8.90E-02
189	BLOOD	24094	2.86E-05	6.88E-01	667	1.06E-03	7.06E-01	62	1.13E-02	6.99E-01
190	CER. SPINAL FL.	6750	2.72E-05	1.84E-01	170	1.01E-03	1.71E-01	19	1.07E-02	2.04E-01
204	EYE (aque.humor)	433	2.72E-05	1.18E-02	13	1.01E-03	1.31E-02	1	1.07E-02	1.07E-02
207	KIDNEYS	12442	2.84E-05	3.53E-01	336	1.05E-03	3.53E-01	29	1.12E-02	3.24E-01
209	BONE MARROW	103047	2.81E-05	2.89E+00	2769	1.04E-03	2.88E+00	251	1.11E-02	2.78E+00
227	BLADDER	3812	2.78E-05	1.06E-01	98	1.03E-03	1.01E-01	9	1.10E-02	9.87E-02
228	TESTICLES	783	2.82E-05	2.21E-02	25	1.04E-03	2.61E-02	1	1.11E-02	1.11E-02
253	BONE (cancellous)	60116	5.18E-05	3.12E+00	1643	1.92E-03	3.16E+00	159	2.04E-02	3.25E+00
256	**All Tissues**	**3799333**	**1.05E+02**	**1.05E+02**	**102634**	**1.05E+02**	**1.05E+02**	**9622**	**1.06E+02**	**1.06E+02**

Figure 4. The ratios between individual organ mass for various voxel sizes (10 vs. 3 mm^3 and 22 vs. 3 mm^3)

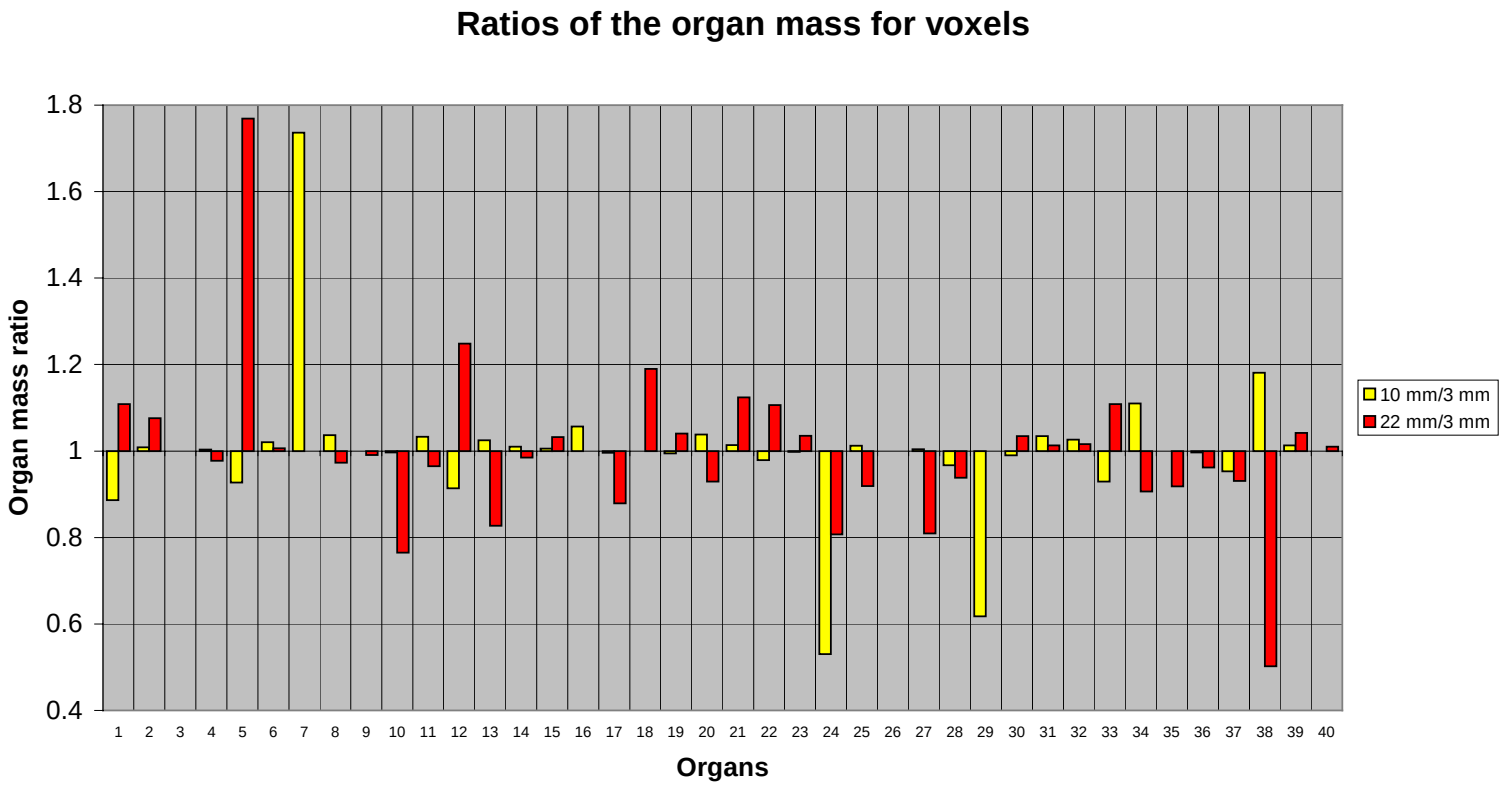

IN	Organ
1	BILE
2	BODY FLUID
3	EYE(cornea)
4	FAT
5	LYMPH
6	MUSC. MEMBRANE
7	NAILS (toe&finger)
8	NERVE (spine)
9	MUSCLE
10	HEART
11	WHITE MATTER
12	STOMACH
13	GLANDS
14	BLOOD VESSEL
15	LIVER
16	GALL. BLADDER
17	SPLEEN
18	CEREBELLUM
19	BONE (cortical)
20	CARTILAGE

IN	Organ
21	LIGAMENTS
22	SKIN/DERMIS
23	INTESTINE (large)
24	TOOTH
25	GRAY MATTER
26	EYE (lens)
27	LUNG (outer)
28	INTESTINE (small)
29	EYE (sclera/wall)
30	LUNG.(inner)
31	PANCREAS
32	BLOOD
33	CER. SPINAL FL.
34	EYE (aque.humor)
35	KIDNEYS
36	BONE MARROW
37	BLADDER
38	TESTICLES
39	BONE (cancellous)
40	All Tissues

Figure 5. Normalized whole body SAR (W/kg per mW/cm^2) values for a man model for selected frequencies and various voxel sizes (3, 10 and 22 mm^3) in EHK orientation. Direction of wave propagation from the dorsal to ventral surface of the man (minus (M) vector).

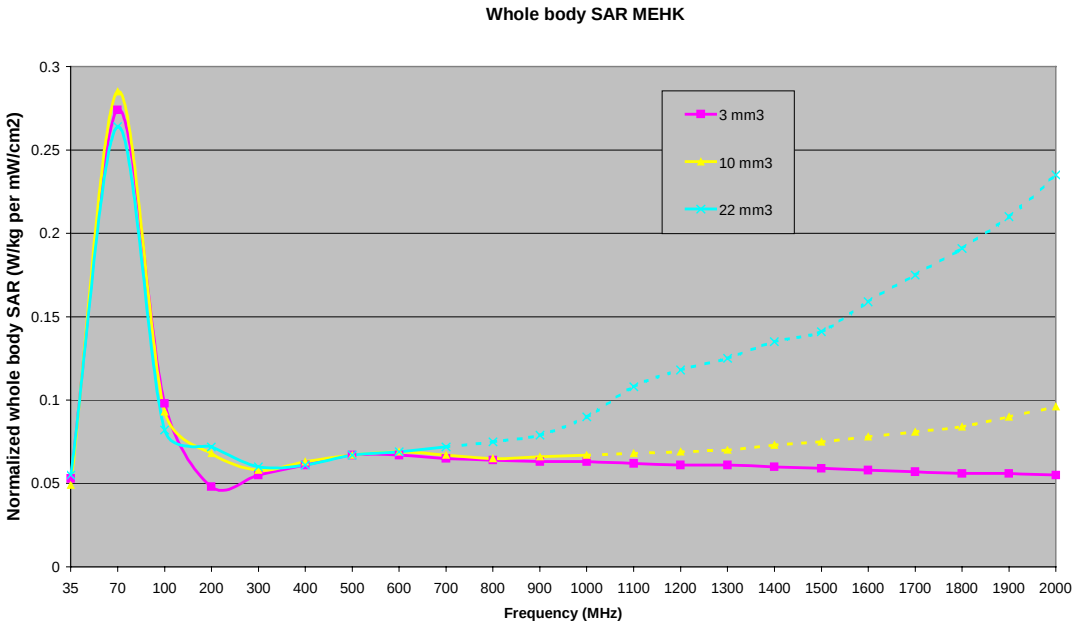

Figure 6. Normalized whole body SAR (W/kg per mW/cm^2) values for a man model for selected frequencies and various voxel sizes (3, 10 and 22 mm^3) in KEH orientation. Direction of wave propagation from the dorsal to ventral surface of the man (minus (M) vector).

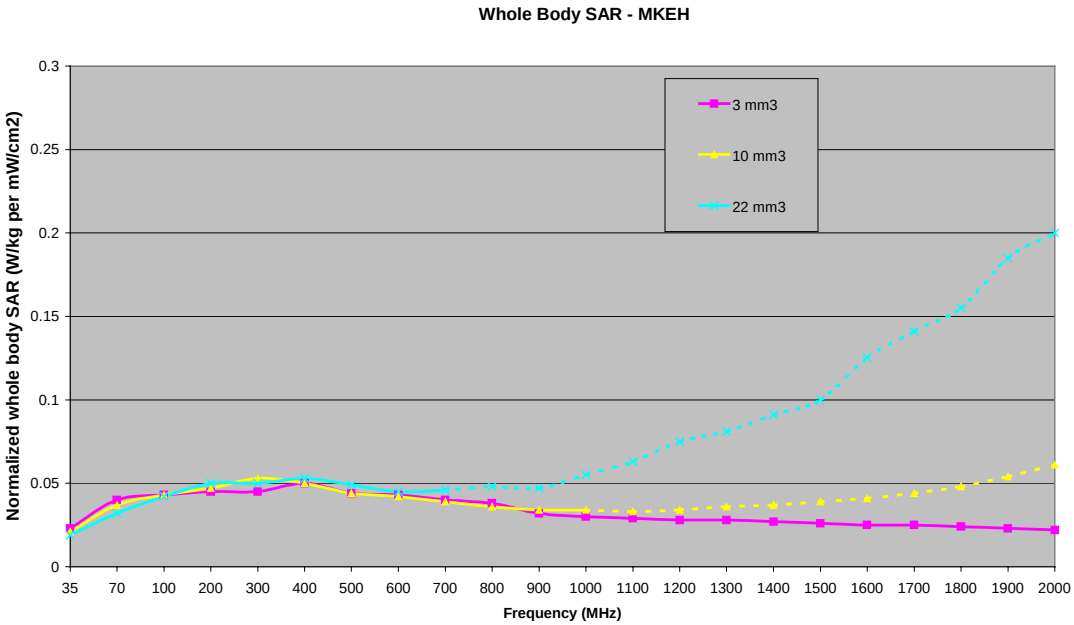

Figure 7. Normalized whole body SAR (W/kg per mW/cm^2) values for a man model for selected frequencies and various voxel sizes (3, 10 and 22 mm^3) in HEK orientation. Direction of wave propagation from the dorsal to ventral surface of the man (minus (M) vector).

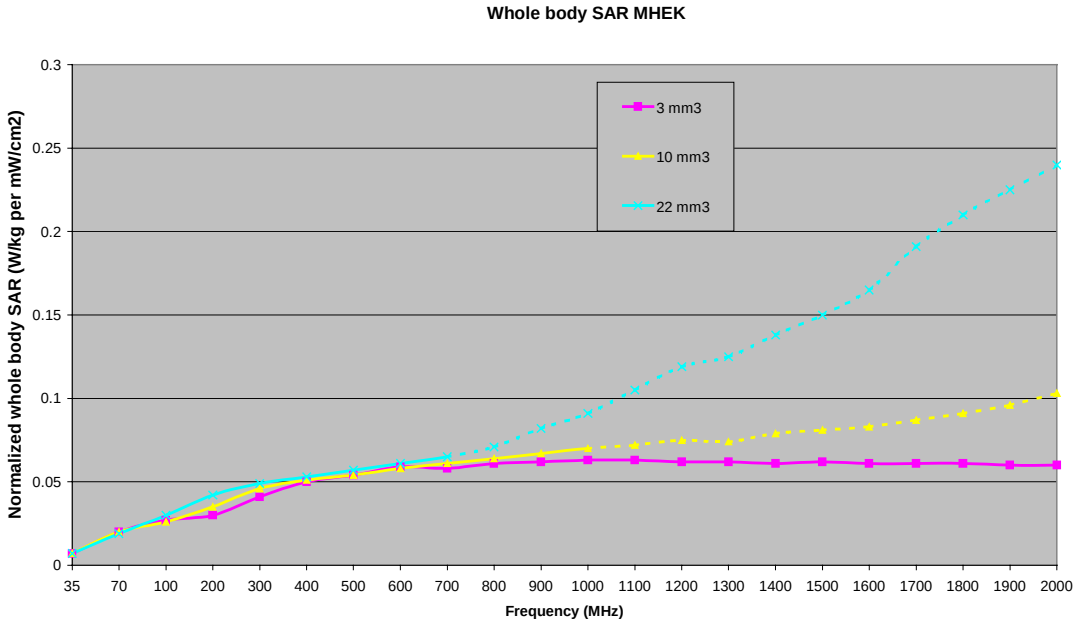

5. DEVELOPMENT OF THE POWER DEPOSITION IN HUMAN TISSUE ALGORITHM - TOOL FOR AVERAGING PROCEDURE (SAR-A-T):

This work contributes towards understanding of the role of various technical approaches in relation to calculate the spatial peak SAR averaged over certain mass of tissue. This satisfies the requirement to quantify the SAR dependence on various model parameters and leads to increased confidence in the validity of the numerical calculations. The basic restriction on the spatial peak SAR averaged over 1 or 10 g tissue mass is set by various international organizations [ICNIRP 1998, IEEE 1999] and regulatory authorities.

One of the objectives of this project is to identify the optimal algorithm for peak spatial SAR averaged over certain mass (1g or 10 g) and to investigate the role of averaging mass procedure on peak spatial averaged SAR. Since various approaches towards the averaging procedures are being investigated [Wang et al. 1999, Caputa et al. 1999, Mason et al. 2000] some technical committees are putting many efforts towards the harmonized technical standard on numerical dosimetry including peak spatial averaging procedures [EN 2001, IEEE 1999],

Besides the above mentioned standardized methodology, some novel techniques for spatial peak SAR averaged over certain mass of a target tissue are being analyzed in this paper. By using these procedures, the most sensitive and critical survival organs where the highest localized SAR versus whole body SAR values, are reported.

A computer algorithm is developed for post processing the FDTD data. The application named *"SAR Averaging Tool (**SAR-A-T**)"* is designed for identification of the spatial peak SAR averaged over 1 or 10 g of tissue. Application is written with ***Delphi*** programming environment. The core of the program represents the basis of the experimental platform that could be easily modified and expanded with new modules. Application is designed as a "console application" with a text window where the user could monitor the current numerical procedures and intermediate results.

Figure 8. Working domain of the application

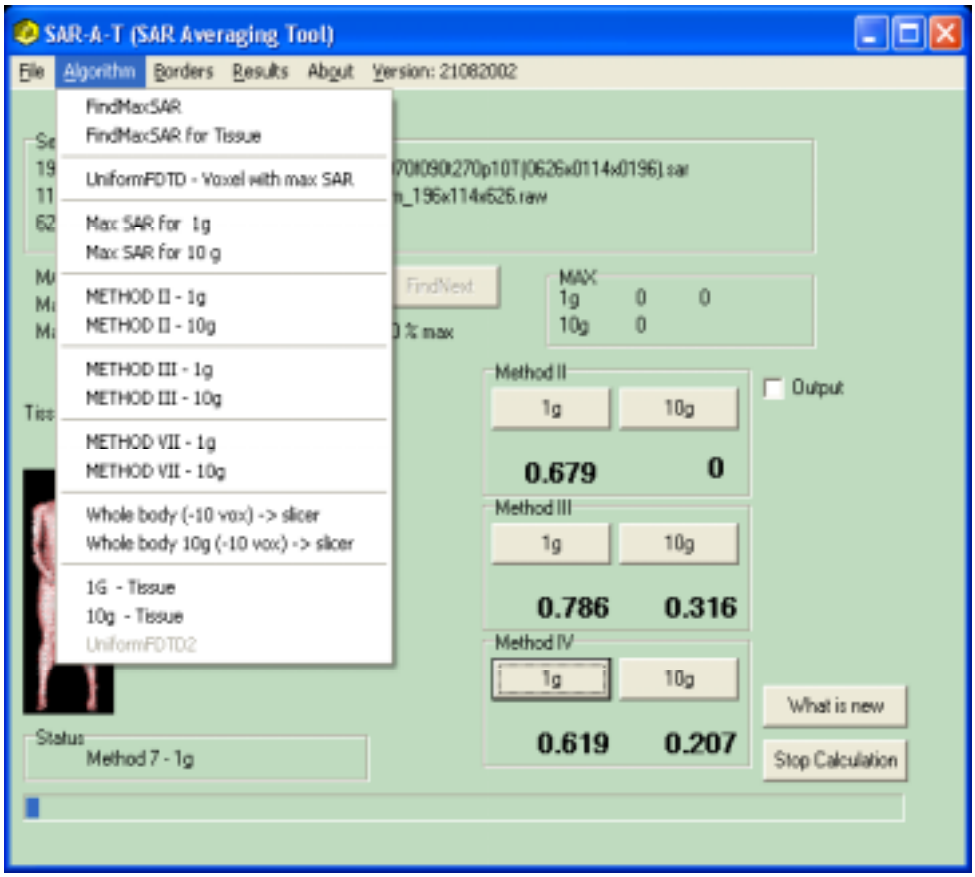

With the use of simple script language (SAR-A-T Script) the calculations are performed automatically. The length of the script is not limited.

Figure 9. SAR-A-T script file

```
TISSFILE
tiss.tiu
RAWFILE
a_man_3mm_196x114x626.raw
SARFILE
MEHK000070f090t270p10T(0626x0114x0196).sar
TISSUE
48
CALCULATION
METHOD7_1G
CALCULATION
METHOD7_10G
....
....
```

BRIEF DESCRIPTION OF THE CORE OF THE ALGORITHM (METHOD I)

In order to find the cube containing the required mass for averaging, a box-shaped volume of voxels surrounding the sampling point (also referred to as the sampling location) is progressively assembled. The sampling point is at the center of a voxel. It represents the averaged spatial-peak SAR value and is assigned the status of the evaluation.

If a cube enclosing the required mass can be found at a sampling point, the corresponding averaged spatial-peak SAR is assigned to it. If a voxel contributes to several averaging operations, the highest spatial peak SAR value is kept as the value at this sampling point.

A sequence of sampling volumes of increasing size (i.e. single voxel 3x3x3 mm) are defined, each centered on the SAR sampling point. Each subsequent volume adds a layer of voxels to the previous one until the enclosed mass is within 5 % of 1 or 10 g. The cubical volume centered at each location (voxel) should be expanded in all directions until desired volume for the required mass is reached with no surface boundary of the averaging volume extending beyond the most exterior surface of the body. For example, when using the 3 mm^3 raster the first layer around the individual voxel consists of 26 voxels, second layer of 98, and third layer of 218. The algorithm is building the layers around the individual voxel until the criterion m <= mref is fulfilled. After this condition is met the difference between mref and m is calculated. The result represents the mass that must be added to the next layer of voxels. Then, mass is being divided with the number of the voxels within the next layer that results in a special correction factor. At the end, the additional condition (m-mRef) < (5%*mRef) must be met.

For illustration, attached is the simplified basic loop of the core algorithm written in pseudo pascal language, where are:

im, jm ,km … the coordinates of the central voxel of the volume,

l…layer counter,

m...mass of the volume,

SAR_AV … Averaged spatial SAR ,

SAR_Sum_V… (sum of the relevant product SAR (I,j,k) * VoxelV(I,j,k))

VoxelV ..volume of the voxel,

V… averaging volume,

```
l:=1
Sar_Sum_V:=0;
V:=0,
repeat
   for i:= im-l to im+l  do
      for j:= jm-l to jm+l do
        for k:= km-l to km+l do
            begin
              VoxelM:=VoxelV* tis[raw[i,j,k]];
              Sar_Sum_V := Sar_Sum + sar[i,j,k]*VoxelV;
              m:=m+VoxelM
              V:=V+ VoxelV;
            end;
l:=l+1;
 until m >= MRef;
 Deltam=m-MRef;
SAR_AV:=Sar_Sum_V/V
```

In each expansion step the percentage of empty voxels (air) is computed to ensure it does not exceed 10 %. If this condition is not satisfied the SAR is considered indeterminate and the algorithm proceeds to the next sampling point.

Current algorithm discards all voxels centered in the volume with more then 10% empty voxels (air). If this criteria is fulfilled, all volumes with at least one face entirely in the air are automatically discarded (for 3 mm^3 resolution and mass 1g or 10g). Described technique for SAR computations is based on a low-pass adaptive 3-D spatial filter. The filter has a cube-shaped mask that changes its volume via an adoption mechanism, responding to changes in the density of tissue (Caputa et al, 1999). From this perspective all voxels in the whole body volume are tested for maximal spatial averaged SAR.

In addition to the above mentioned routine for calculating peak spatial SAR anywhere in the body, three various methods have been developed to identify the spatial peak averaged SAR for individual tissue/organ.

Method II (averaged spatial SAR around a voxel with peak SAR for selected tissue)

First, the individual voxel with the maximal SAR for the selected tissue/organ must be found. Than, the corresponding number of layers are added to that centered voxel to achieve the desired mass (1 g or 10 g). Out of this volume, only selected tissue type or organ is taken into consideration when calculation the averaging SAR value. We use the same procedure as described for the core algorithm, with additional parameter for the tissue code.

For simplified example: (procedure Calc_SAR_AV_M1 has many other parameters not shown in this example)

```
procedure Calc_SAR_AV_M1(imax,jmax,kmax: integer; MRef:double; tissue:integer;...

    /if tissue is 0 all voxels are included, (only empty voxels are not included)
    /if tissue is 1..255 then only voxels with this tissue code are included

    /for example _SAR_AV_M1 (253,….) calculates SARaverage only for bones
```

Method III (Absolute spatial peak SAR for selected tissue regardless of No. of voxels**)**

This method is based on the same procedure as Method I described for the core algorithm with additional parameter for the tissue code. It is based on a low-pass adaptive 3-D spatial filter. The filter has a cube-shaped mask that changes its volume via an adoption mechanism, responding to changes in the density of tissue. The selected volume (1g or 10g), which could spread up to the 10000 voxels, considers only voxels of selected tissue/organ ID. Current method discards all voxels centered in the volume with more then 10% empty voxels (air). The result represents the spatial peak SAR for the chosen tissue/organ regardless of the combination between the spatial distribution of the voxels with the same tissue/organ IN and the total number of the used voxels in the procedure.

Method IV (Absolute spatial peak SAR for selected tissue considering the of No. of voxels)

When looking for the localized hot spots in individual tissue/organ the method considering the smallest area for the averaging should be developed. The **SAR-A-T** method IV is, in fact, very similar to the **SAR-A-T** method III with different endpoint. It looks for the maximal ratio between the spatial peak averaged SAR value in particular tissue/organ and the number of the used voxels continuously. Thus, the cube containing the required mass with the smallest extension (smallest number of the corresponding voxels of the chosen tissue/organ) is taken for the evaluation of the spatial peak SAR.

Figure 10. Calculation results are written in the console window and in the log file

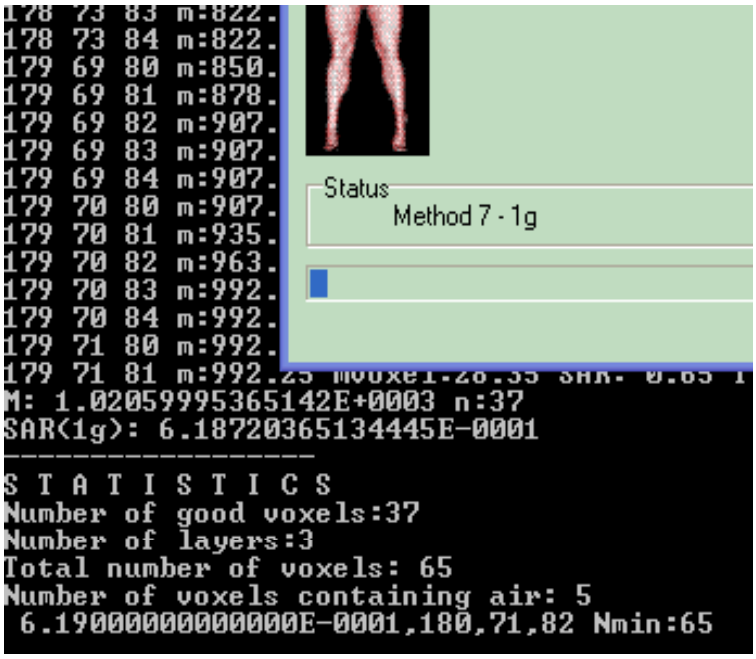

This particular method seems to be the most appropriate for calculating the peak spatial averaged SAR throughout the entire individual tissue/organ by optimizing the selected area for searching the voxels with the highest SAR values.

6. INTER-COMPARISON OF THE SPATIAL PEAK SAR VALUES FOR VARIOUS VOXEL SIZES AND AVERAGING MASS INTERVALS

Since the predicted normalized whole body SAR average is not substantially influenced by the size of the voxel in the used model (3, 10 or 22 mm^3), the major emphasis was given to the variability in spatial peak SAR values when using various voxel sizes of the digital anatomical model and various mass intervals (1 g and 10 g).

First, the existing voxel size of the 3 mm^3 man was changed in such a way that mass of the voxel corresponds to the standardized averaging mass interval (1g requires voxel size of 10 mm^3, 10 g requires voxel size of 21.5 mm^3). These modified digital models were used as an input to FDTD code. We have examined three various orientations and various frequencies. Second, the SAR data obtained by original voxel size of the man model (3 mm^3) were used as an input to the core of the SAR_AT algorithm. According to the methodology described in previous chapter, the newly developed software tool was applied to calculate the spatial peak SAR (W/kg per mW/cm^2) averaged over 1 g and 10 g of tissue for various exposure conditions.

Results of our study clearly demonstrate that spatial peak SAR values are substantially higher when using smaller voxel size (10 mm^3 - 1 g of the tissue) of the man in comparison to the bigger voxel size (22 mm^3 -10 g of the tissue). This is in good agreement with general understanding of the RF dosimetry principles as well as with data demonstrated by Mason et al. [2000] and Gandhi et al. [2000]. Lin [2000] reported that localized SAR averaged in 10 g could be as much as five times lower (or more lenient) than those obtained by averaging over 1 g of tissue.

The maximum ratios between spatial peak SAR and whole body SAR average reach relatively high values (up to 75 for 22 mm^3 and 59 for 10 mm^3 – MHEK, around 39 for 22 mm^3 and 63 for 10 mm^3 – MKEH and 37 for 22 mm^3 and 85 for 10 mm^3 – MEHK). The results of the absolute spatial peak SAR values and ratios between spatial peak SAR and whole body SAR for individual frequency and orientation for different resolution of the man model are presented in the Tables 2-5.

Somewhat lower ratios were found in 3mm^3 resolution man model when calculating peak spatial SAR averaged over 1g or 10g (up to 46 for 10 g and 64 for 1 g – MHEK, up to 40 for 10 g and 42 for 1 g – MKEH and 36 for 10 g and 53 for 1 g – MEHK). The results of the absolute spatial peak SAR values and ratios between spatial peak SAR and whole body SAR for individual frequency and orientation for different resolution of the man model are presented in the Tables 6-9.

The detailed analysis of the spatial peak SAR averaged over 1g of 10g for 70 MHz, MEHK orientation shows that the highest value appeared to be in the ankle region. In contrast to the results obtained by using

coarser models (10 and 22 mm^3), the spatial peak SAR in 3 mm^3 man model reached substantially lower values for both averaging mass intervals (see Figure 11). Similar trend was observed in some other parts of the body —white matter (head) whereas the differences were not so substantial. This could be due to the lower localized SAR values versus whole body SAR average in the brain region (see Figure 12).

As the voxel size increases (10 and 22 mm^3) small organs may be distorted or lost, some symmetries may be affected, organs will change mass slightly and the continuity of elongated structures may be disrupted. According to these observations it could be concluded that low resolution anatomical models don't offer satisfactory and precise information on localized distribution of the absorbed energy in tissues. Furthermore, coarser anatomical models that in perspective converge to homogenous models offer a kind of worst case scenario and overpredict the spatial peak SAR average.

Table 2. Spatial peak SAR (W/kg per mW/cm^2) for MKEH orientation and various frequencies for 22 mm^3 and 10 mm^3 voxel size of the modified man model, respectively. In addition, the corresponding tissue/organ with spatial peak SAR is reported.

Frequency	22 mm MKEH		10 mm MKEH	
(MHz)	spatial peak (*)	organ	spatial peak (*)	organ
70.00	0.97	muscle	1.15	muscle
100.00	1.40	muscle	1.61	muscle
200.00	1.70	muscle	1.95	muscle
300.00	1.58	muscle	2.10	muslce
400.00	1.59	muscle	1.68	muscle
500.00	1.34	muscle	1.50	fat
600.00	1.12	ligaments	1.84	muscle
700.00	1.29	ligaments	2.46	fat
800.00			1.60	muscle
900.00			1.64	skin
1000.00			2.00	skin

(*) – spatial peak SARs are listed in W/kg per mW/cm^2

7

Table 3. Spatial peak SAR (W/kg per mW/cm^2) for MEHK orientation and various frequencies for 22 mm^3 and 10 mm^3 voxel size of the modified man model, respectively. In addition, the corresponding tissue/organ with spatial peak SAR is reported.

Frequency	22 mm MEHK		10 mm MEHK	
(MHz)	spatial peak (*)	organ	spatial peak (*)	organ
70.00	9.87	muscle	17.50	fat
100.00	1.88	muscle	2.64	muscle
200.00	2.18	muscle	2.56	muscle
300.00	1.22	muscle	2.38	fat
400.00	1.40	muscle	2.80	fat
500.00	2.18	muscle	5.71	fat
600.00	2.40	muscle	4.30	fat
700.00	1.80	muscle	3.76	muscle
800.00			3.10	skin
900.00			4.31	skin
1000.00			5.12	skin

(*) – spatial peak SARs are listed in W/kg per mW/cm^2

Table 4. Spatial peak SAR (W/kg per mW/cm^2) for MHEK orientation and various frequencies for 22 mm^3 and 10 mm^3 voxel size of the modified man model, respectively. In addition, the corresponding tissue/organ with spatial peak SAR is reported.

Frequency	22 mm MHEK		10 mm MHEK	
(MHz)	speatial peak (*)	organ	spatial peak (*)	organ
70.00	1.05	skin	1.00	skin
100.00	2.25	skin	1.55	skin
200.00	2.07	skin	1.32	skin
300.00	1.31	skin	1.40	skin
400.00	0.89	skin	2.56	muscle
500.00	1.21	skin	1.81	fat
600.00	1.20	skin	2.68	fat
700.00	1.97	ligaments	2.70	skin
800.00			2.73	fat
900.00			3.54	skin
1000.00			4.17	skin

(*) – spatial peak SARs are listed in W/kg per mW/cm^2

Table 5. Ratios between spatial peak SAR and whole body SAR average for all applied orientations and frequencies for 22 mm^3 and 10 mm^3 voxel size of the modified man model.

Frequency (MHz)	MEHK 22 mm	MEHK 10 mm	MKEH 22 mm	MKEH 10 mm	MHEK 22 mm	MHEK 10 mm
70.00	37.39	61.40	30.31	31.08	55.26	50.00
100.00	22.93	28.39	33.33	37.44	75.00	59.62
200.00	30.28	37.65	34.00	41.49	49.29	37.71
300.00	20.33	41.03	31.60	39.62	26.73	30.43
400.00	22.95	44.44	30.00	33.60	16.79	50.20
500.00	32.54	85.22	27.35	34.09	21.23	33.52
600.00	34.78	62.32	24.89	43.81	19.67	46.21
700.00	25.00	56.12	28.04	63.08	30.31	44.26
800.00		47.69		44.44		42.66
900.00		65.30		48.24		52.84
1000.00		76.42		58.82		59.57

Table 6. Spatial peak SAR (W/kg per mW/cm^2) averaged over 1 g and 10 g for MEHK orientation and various frequencies for 3 mm^3 voxel size of the man model. In addition, the corresponding tissue/organ with spatial peak SAR is reported.

MEHK Orientation – 3 mm3 voxel size				
Frequency (MHz)	**spatial peak SAR 1 g average**	**organ**	**spatial peak SAR 10 g average**	**organ**
70.00	10.37	muscle	7.06	musc
100.00	2.17	muscle	1.66	musc
200.00	1.33	cer.fluid	0.90	cer.fluid
300.00	1.63	muscle	1.09	skin
400.00	1.54	muscle	1.07	muscle
500.00	3.68	muscle	2.51	skin
600.00	2.73	muscle	1.88	muscle
700.00	2.55	muscle	1.46	muscle
800.00	1.38	muscle	1.05	muscle
900.00	1.28	muscle	0.91	muscle
1000.00	1.11	muscle	0.86	muscle
1100.00	1.28	muscle	0.86	muscle
1200.00	1.47	muscle	0.96	fat
1300.00	1.56	muscle	0.87	muscle
1400.00	1.49	muscle	0.94	muscle
1500.00	1.64	fat	1.08	muscle
1600.00	1.96	ligaments	1.13	skin
1700.00	2.28	fat	1.26	skin
1800.00	1.98	ligaments	1.16	skin
1900.00	1.73	muscle	1.04	muscle
2000.00	1.78	skin	0.99	muscle

(*) – spatial peak SARs are listed in W/kg per mW/cm^2

Table 7. Spatial peak SAR (W/kg per mW/cm^2) averaged over 1 g and 10 g for MHEK orientation and various frequencies for 3 mm^3 voxel size of the man model. In addition, the corresponding tissue/organ with spatial peak SAR is reported.

MHEK Orientation – 3 mm3 voxel size				
Frequency (MHz)	**spatial peak SAR** 1 g averaged	**organ**	**spatial peak SAR** 10 g averaged	**organ**
70.00	1.41	fat	0.98	skin
100.00	2.20	fat	1.40	skin
200.00	1.04	fat	0.75	skin
300.00	0.49	fat	0.57	skin
400.00	0.96	muscle	0.56	muscle
500.00	1.05	skin	0.71	muscle
600.00	1.14	muscle	0.88	muscle
700.00	1.73	muscle	1.29	fat
800.00	1.79	muscle	1.35	muscle
900.00	1.47	muscle	1.09	muscle
1000.00	1.84	muscle	1.21	muscle
1100.00	2.14	muscle	1.43	muscle
1200.00	2.10	muscle	1.51	muscle
1300.00	1.74	muscle	1.37	muscle
1400.00	1.37	muscle	1.10	muscle
1500.00	1.26	fat	1.07	muscle
1600.00	1.44	fat	1.13	muscle
1700.00	1.60	fat	1.27	muscle
1800.00	1.63	fat	1.29	muscle
1900.00	1.54	fat	1.16	muscle
2000.00	1.41	fat	1.03	muscle

(*) – spatial peak SARs are listed in W/kg per mW/cm^2

Table 8. Spatial peak SAR (W/kg per mW/cm^2) averaged over 1 g and 10 g for various exposure conditions for 3 mm^3 voxel size of the man model. In addition, the corresponding tissue/organ for spatial peak SAR is reported.

MKEH Orientation – 3 mm3 voxel size				
Frequency (MHz)	**spatial peak SAR** 1g averaged	**organ**	**spatial peak SAR** 10 g averaged	**organ**
70.00	0.95	bone	0.69	muscle
100.00	1.30	muscle	0.80	muscle
200.00	0.98	muscle	0.63	muscle
300.00	1.72	muscle	0.50	skin
400.00	1.20	muscle	0.89	muscle
500.00	1.00	fat	0.60	fat
600.00	1.10	muscle	0.70	skin
700.00	0.85	muscle	0.86	muscle
800.00	0.96	muscle	0.60	muscle
900.00	0.67	muscle	0.45	ligament
1000.00	0.65	muscle	0.60	muscle
1100.00	1.20	muscle	0.75	muscle
1200.00	1.10	muscle	0.74	muscle
1300.00	0.91	muscle	0.70	muscle
1400.00	1.00	muscle	1.00	muscle
1500.00	0.95	fat	0.70	muscle
1600.00	0.85	fat	0.68	skin
1700.00	1.10	muscle	0.65	muscle
1800.00	0.90	fat	0.65	muscle
1900.00	0.85	muscle	0.70	muscle
2000.00	1.00	skin	0.60	skin

(*) – spatial peak SARs are listed in W/kg per mW/cm^2

Table 9. Ratios between spatial peak SAR averaged over 1g and 10 g and whole body SAR average for various exposure conditions for 3 mm^3 voxel size of the man model.

Frequency	MEHK	MEHK	MKEH	MKEH	MHEK	MHEK
(MHz)	1 g	10 g	1 g	10 g	1 g	10 g
70	38.4	26.2	23.8	17.3	64.1	44.5
100	19.7	15.1	31.0	19.0	73.3	46.7
200	33.3	22.5	22.8	14.5	32.5	23.5
300	27.2	18.1	39.1	11.4	11.9	13.9
400	22.0	15.3	24.0	17.8	19.1	11.2
500	53.3	36.4	22.2	13.3	20.6	14.0
600	40.1	27.6	27.5	17.5	21.5	16.6
700	38.1	21.8	23.0	23.2	32.1	23.9
800	21.2	16.2	28.2	17.6	32.0	24.1
900	19.7	14.0	22.3	15.0	24.5	18.2
1000	17.3	13.4	22.4	20.7	28.3	18.6
1100	20.6	13.9	42.9	26.8	32.9	22.0
1200	24.5	16.0	40.7	27.4	32.3	23.2
1300	26.0	14.5	35.0	26.9	27.2	21.4
1400	24.9	15.7	40.0	26.0	21.4	17.2
1500	28.3	18.6	39.6	29.2	19.7	16.7
1600	34.4	19.8	35.4	28.3	22.5	17.7
1700	40.7	22.5	47.8	28.3	25.0	19.8
1800	36.0	21.1	40.9	29.5	25.5	20.2
1900	32.0	19.3	38.6	31.8	24.1	18.1
2000	33.0	18.3	40.0	24.0	22.4	16.3

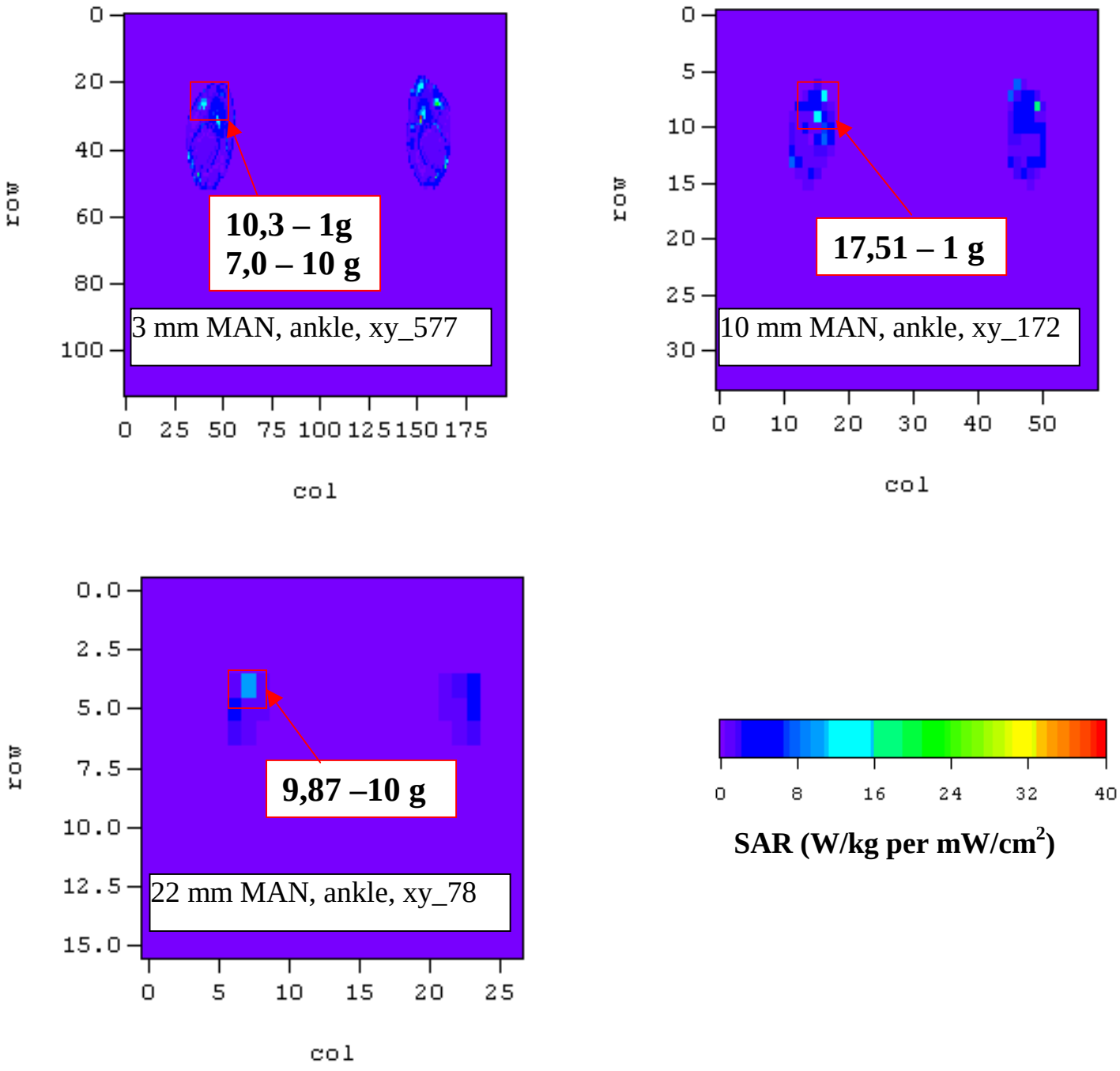

Figure 11. Spatial peak SAR for three various voxel sizes (3, 10 and 22 mm^3) at resonant frequency (70MHz) at MEHK orientation. In all used man models the peak SAR was found in an ankle region.

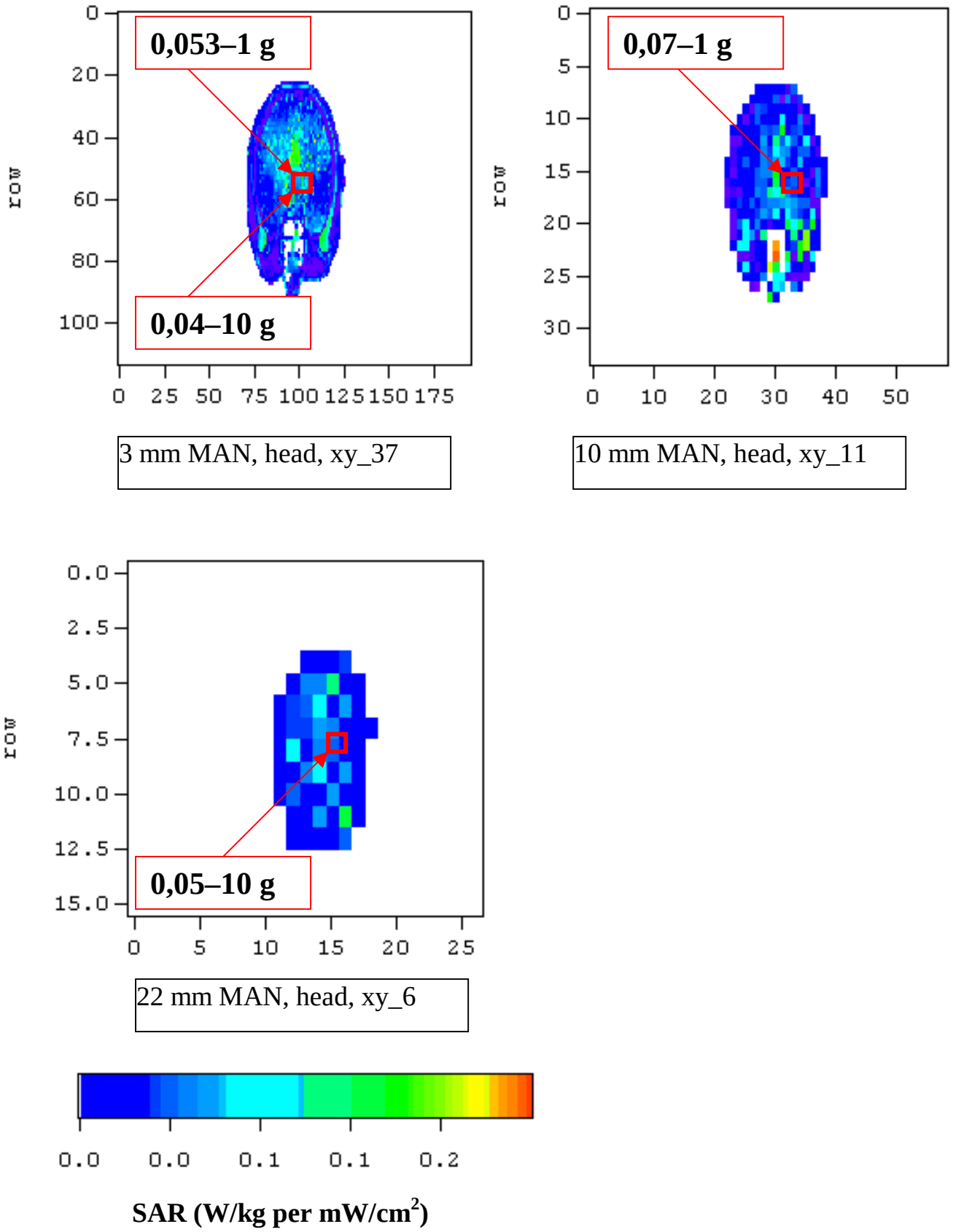

Figure 12. Spatial peak SAR for three different voxel sizes (3, 10 and 22 mm^3) at resonant frequency (70MHz) at MEHK orientation. The spatial peak SAR is compared in the brain - gray matter.

7. SPATIAL PEAK SAR IN CRITICAL SURVIVAL ORGANS

When the power absorption takes place in a confined body region, the localized SAR can assume rather high values, even if the whole body SAR is relatively low. The localized SAR values are dependent on specific exposure conditions and could be higher by several orders of magnitude [Hurt 2000]. Thus, whole-body SAR should not be the only criteria used for dose-response evaluations of RF effects. Information about the location of maximal RF absorption inside the body and, thus, the most affected organ or tissue for various exposure conditions (frequency, orientation) is essential. More detailed analysis of variations in localized SAR in target organs of primary interest (heart, lung, brain, liver, muscle…) in relation to various range of organ sizes and shapes, frequencies, and orientations is needed. High SAR values near blood vessels may be less consequential than a high SAR deep in muscle, whereas high SAR in muscle tissue may be less consequential than high SAR in lung tissue or nerves. Thus, the localized SAR values in the brain and spinal cord seem to be more appropriate parameter for risk assessment than the whole body SAR [Chou et al. 1996].

To identify the peak localized SAR value in each individual tissue/organ averaged over certain mass intervals, various techniques for altered exposure conditions (frequency, orientation) were investigated during present project. The methods used for calculating spatial peak SAR are fully described in chapter 5.

Further, peak localized SAR in critical tissues/organs averaged over various masses were compared to whole body SAR average. Inter-comparison of the data represents a basis for setting criteria for more accurate numerical dosimetry or even for setting the appropriate ratio between whole body and localized SAR in health and safety standards. Localized resonance of individual target tissue/organ is important when considering relationship between average SAR and variety in exposure conditions. The focus is on localized SAR values in critical survival organs (white and gray matter, heart, inner and outer lung, liver, muscle, cerebral spinal fluid, nerve spinal, heart) in relation to various frequencies and orientations. This parametric study investigates the highest ratio between the peak localized and whole body SAR average.

Three kinds of averaging procedures for 1 g and 10 g averaged spatial peak SAR for individual tissue/organ have been introduced (**method II, III and IV;** for details see chapter 5) and their uncertainties have been evaluated. The results have shown that an uncertainty between 1.2 and 2.0 times may exists at certain frequency and orientation, depending on used method. Generally speaking, when applying the **Method III** the highest ratios between spatial peak SAR and whole body SAR average in all selected tissues/organs were found. **Method II** showed similar pattern but somewhat lower ratios. The most interesting approach offers **Method IV** where the spatial peak SAR is related to the smallest selected valid volume and, thus, the data are

expected to be reliable with local hot spots. The results obtained by this method also offer the basis for interpretations and conclusions about the spatial peak in the critical survival organs.

All three methods are presented in Figures from 13 to 21 showing the ratios between peak localized SAR and whole body SAR average for selected tissues for various mass intervals (1g and 10 g), orientations (MEHK; MHEK, MKEH) and frequencies (70-2000 MHz). The present work demonstrated that frequency dependent ratios between spatial peak SAR and whole body SAR average show quite similar pattern for all applied methods (III, II and IV) but various absolute values.

We found the highest absolute SAR value (10.3 W/kg per mW/cm^2 averaged over 1 g and 7 W/kg per mW/cm^2 averaged over 10 g) as well as highest ratio (over 40) for muscle at resonant frequency (70 MHz) at MEHK orientation. According to presented data, the muscle seems to be the primary site of interaction where the great majority of incident RF energy is absorbed. Several other peaks were found around 600 MHz and 1800 MHz, respectively. At MKEH and MHEK orientations, lower values with no significant maximum are reported (see Figure 13).

When comparing with muscle, relatively lower absolute SAR values and ratios between spatial peak SAR and whole body SAR average were observed in other selected tissues. These ratios for cerebral spinal fluid and nerve spinal were close to 30 at 200 MHz and 15 at 70 MHz at MEHK orientation, respectively. At MKEH and MHEK orientations, lower ratios were observed. The absolute spatial peak SAR values averaged over 1g and 10g are presented in the Tables14 and 15. Energy absorption within the brain (gray matter, white matter) was something lower and has reached its maximal value at MKEH orientation between 600-1000 MHz. The maximal ratios between peak localized SAR and whole body SAR were around 10 (see Figure 16 and 17). In contrast, relatively low ratios between spatial peak SAR and whole body SAR average were found in heart, liver, lung outer and lung inner (between 3 and 7) (see Figures 18 to 21).

When choosing 1 g averaging volume, the ratios between spatial peak and whole body SARs anywhere in the body were normally much higher than factor of 20. On the other hand, the ratios obtained by 10 g averaging volume were close to factor of 20. This was particularly true for muscle, skin, cerebral spinal fluid and fat. For other critical survival organs, the ratios between spatial peak and whole body SARs obtained by both averaging volumes were lower than 20.

Figure 13. Ratios between peak localized SAR and whole body SAR average for muscle for various mass intervals (1g and 10 g), orientations (MEHK; MHEK, MKEH) and frequencies (70-2000 MHz) by considering three various methods (algorithm).

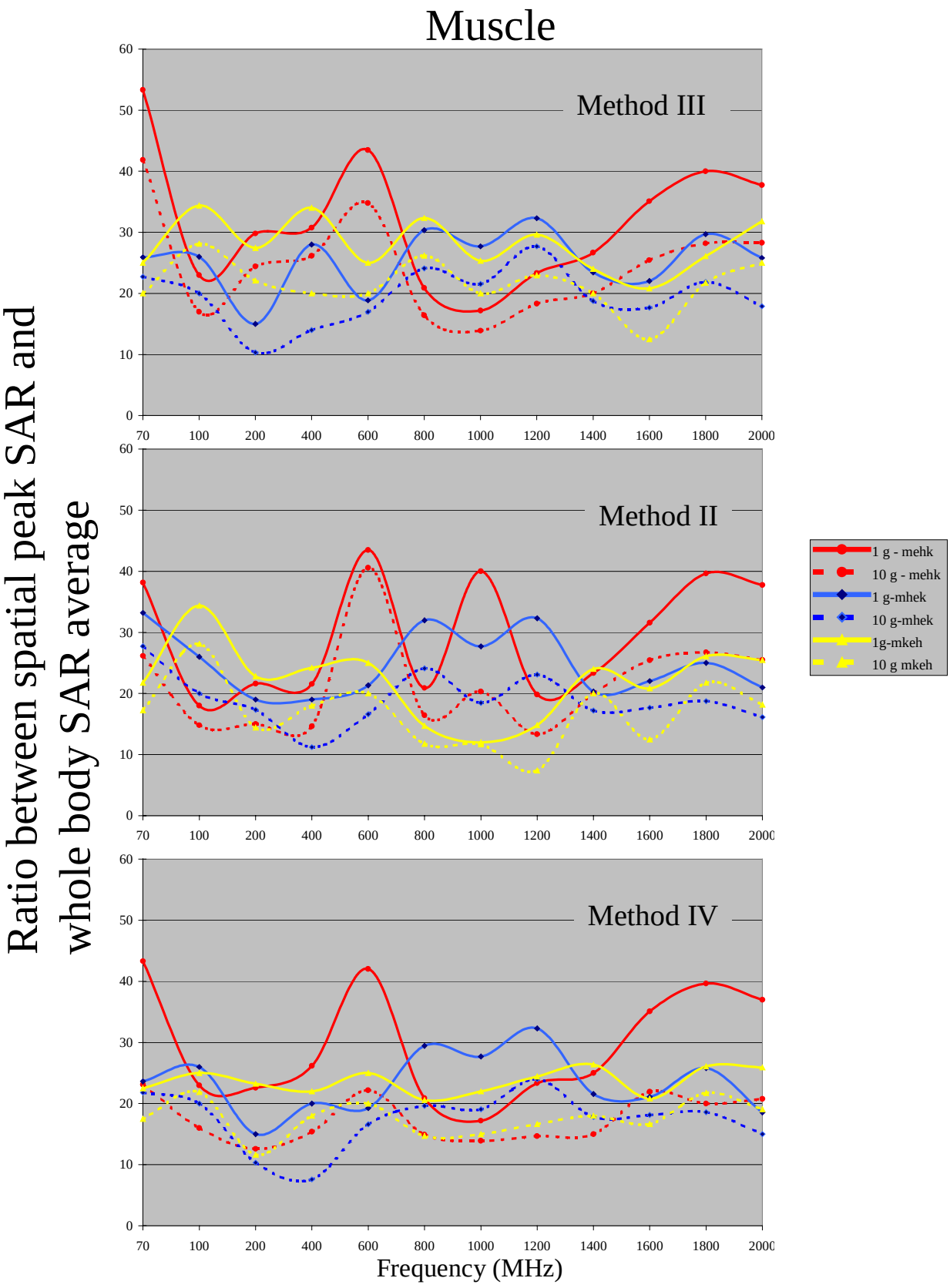

Figure 14. Ratios between peak localized SAR and whole body SAR average for nerve spinal for various mass intervals (1g and 10 g) orientations (MEHK; MHEK, MKEH) and frequencies (70-2000 MHz) by considering three different methods (algorithm).

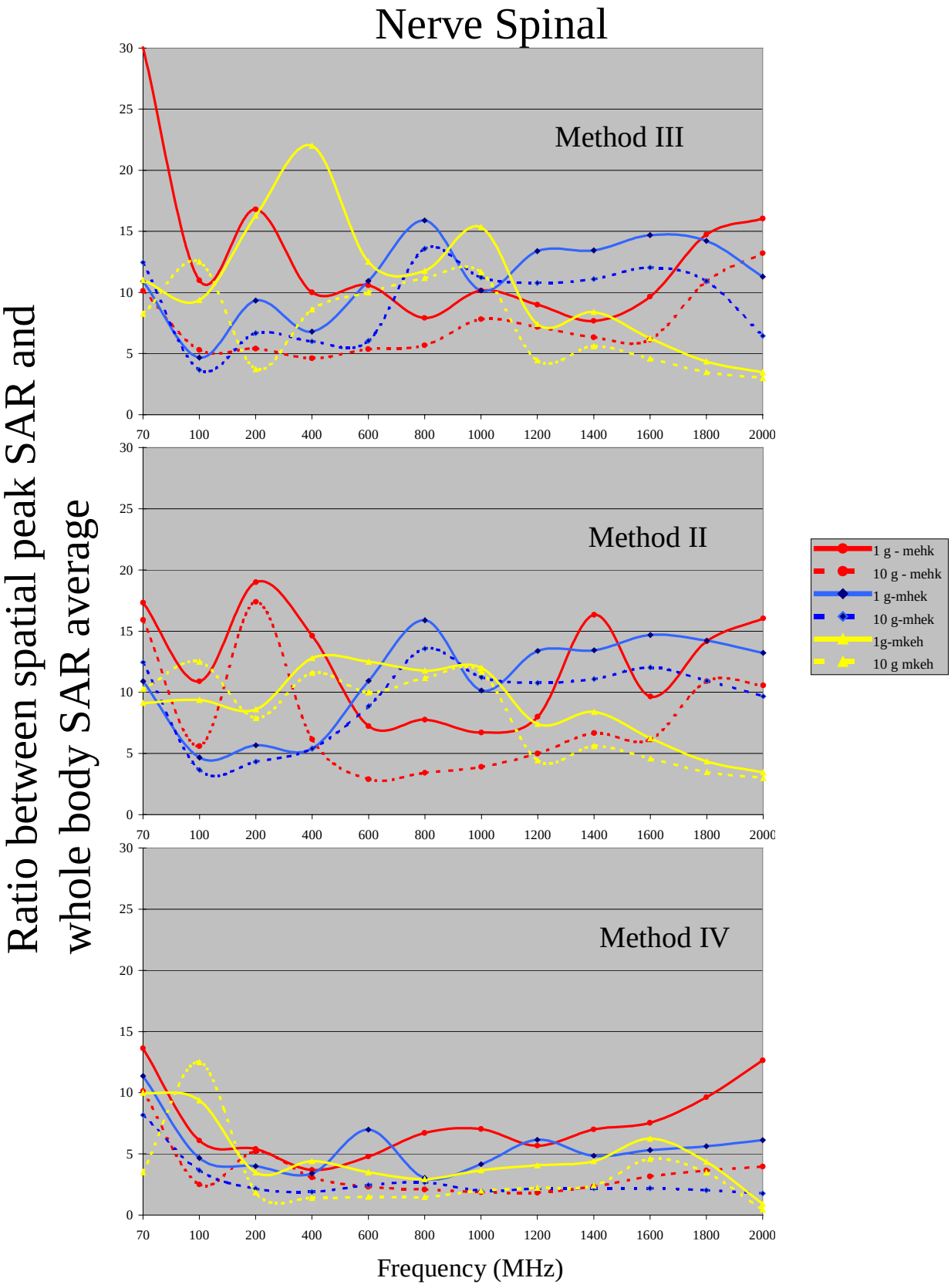

Figure 15. Ratios between peak localized AR and whole body SAR average for cerebral spinal fluid for various mass intervals (1g and 10 g), orientations (MEHK; MHEK, MKEH) and frequencies (70-2000 MHz) by considering three different methods (algorithm).

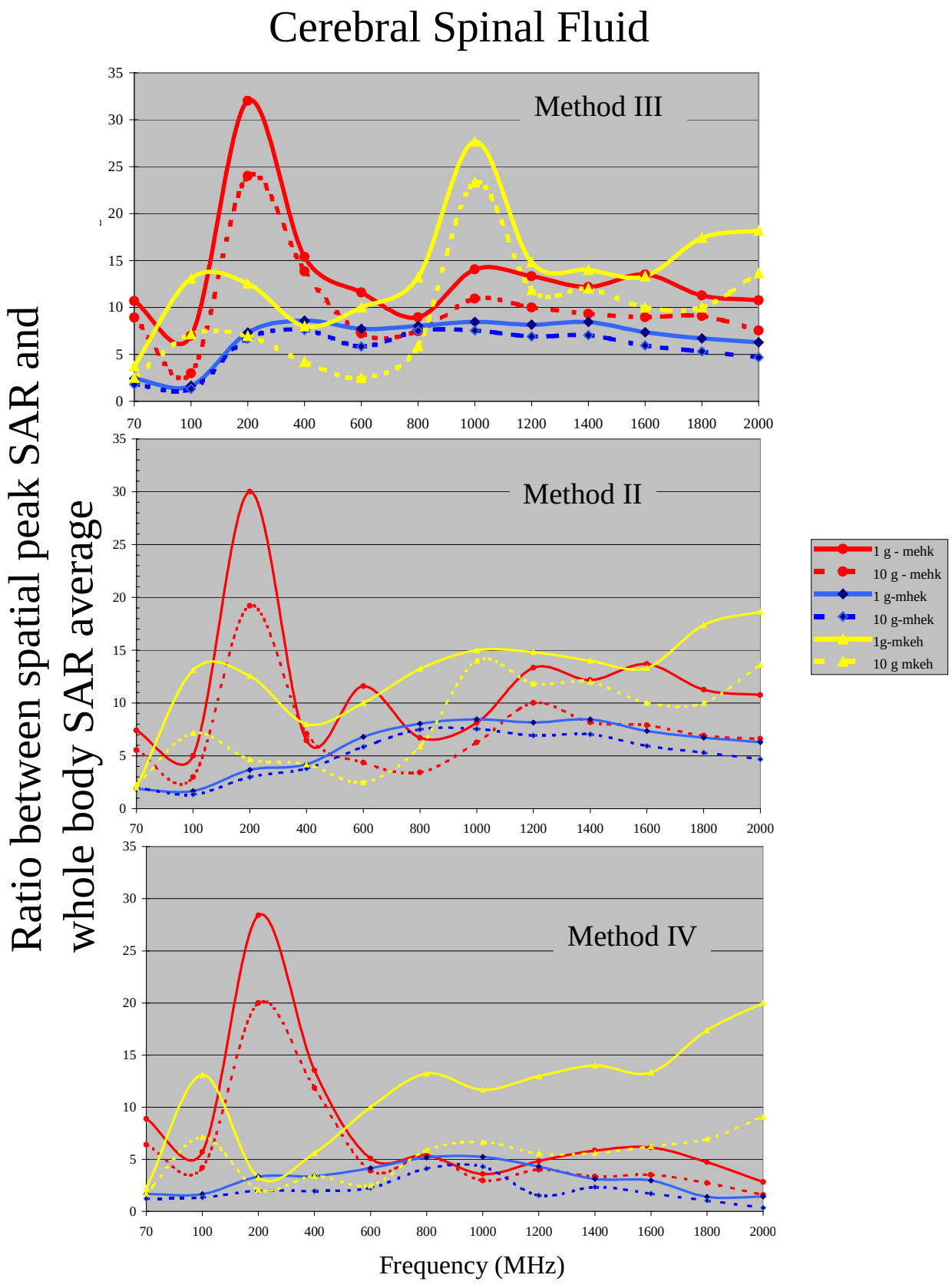

Figure 16. Ratios between peak localized SAR and whole body SAR average for gray matter for various mass intervals (1g and 10 g), orientations (MEHK; MHEK, MKEH) and frequencies (70-2000 MHz) by considering three different methods (algorithm).

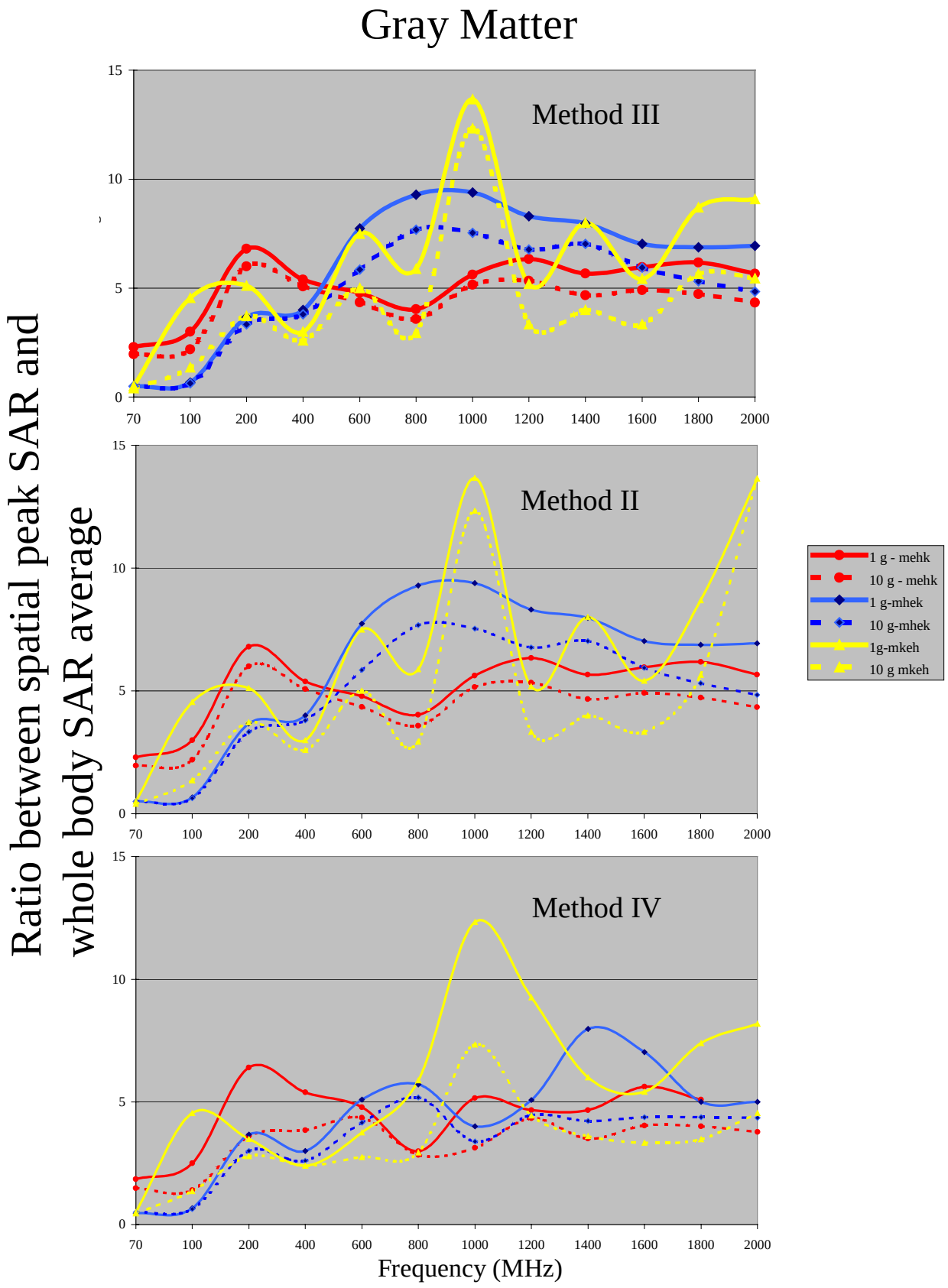

Figure 17. Ratios between peak localized SAR and whole body SAR average for white matter for various mass intervals (1g and 10 g), orientations (MEHK; MHEK, MKEH) and frequencies (70-2000 MHz) by considering three different methods (algorithm).

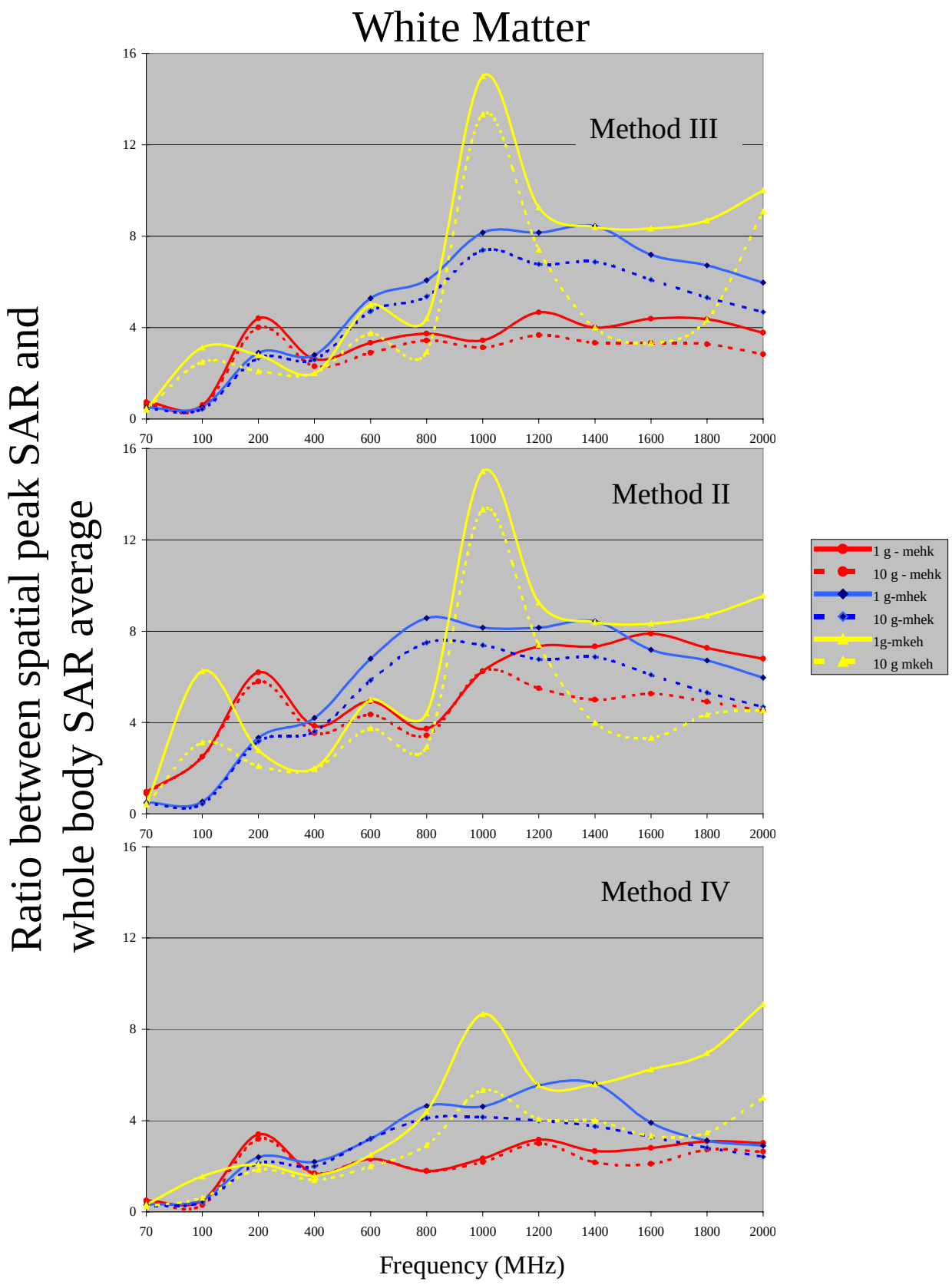

Figure 18. Ratios between peak localized SAR and whole body SAR average for heart for various mass intervals (1g and 10 g), orientations (MEHK; MHEK, MKEH) and frequencies (70-2000 MHz) by considering three different methods (algorithm).

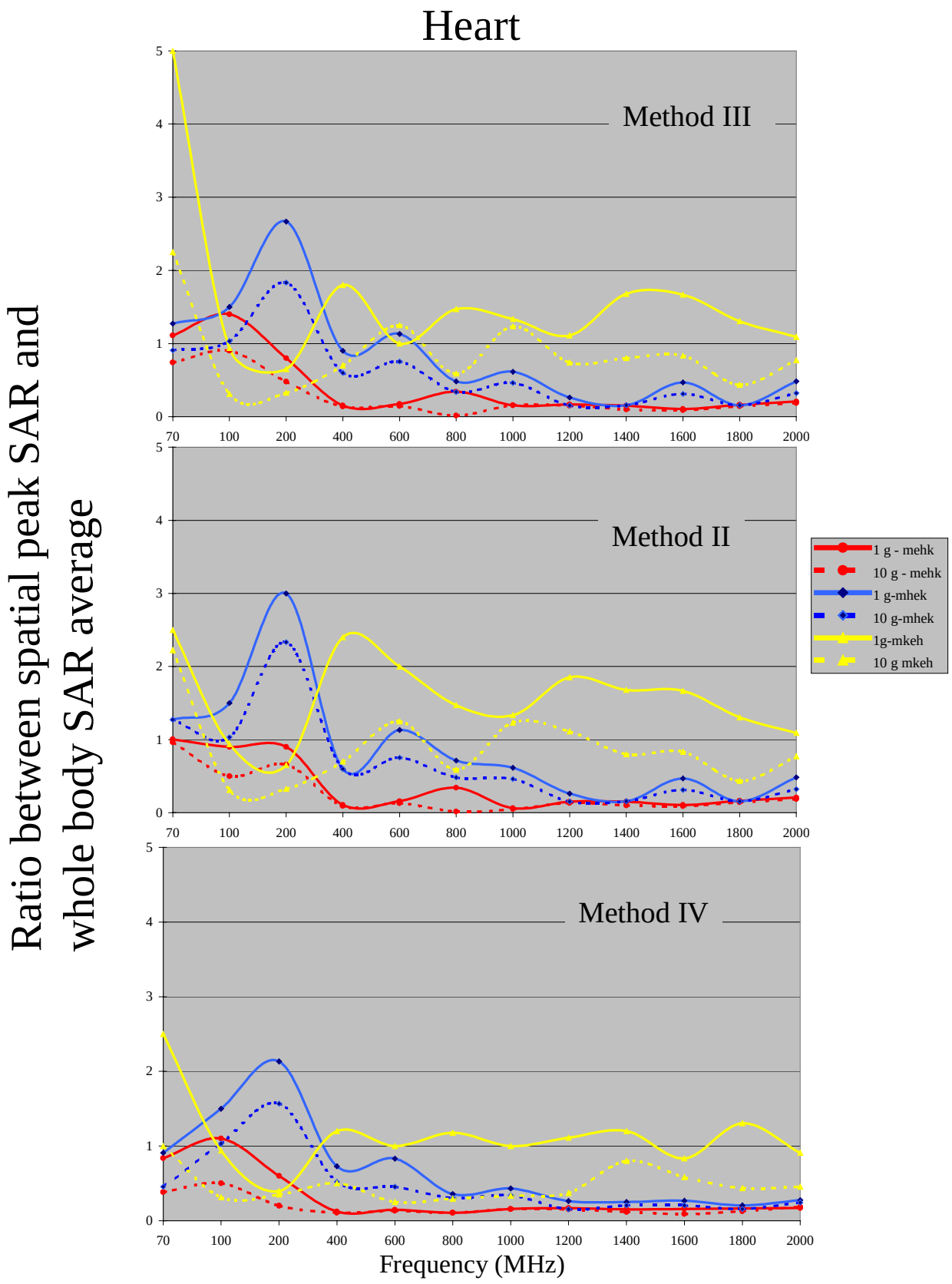

Figure 19. Ratios between peak localized SAR and whole body SAR average for liver for various mass intervals (1g and 10 g), orientations (MEHK; MHEK, MKEH) and frequencies (70-2000 MHz) by considering three different methods (algorithm).

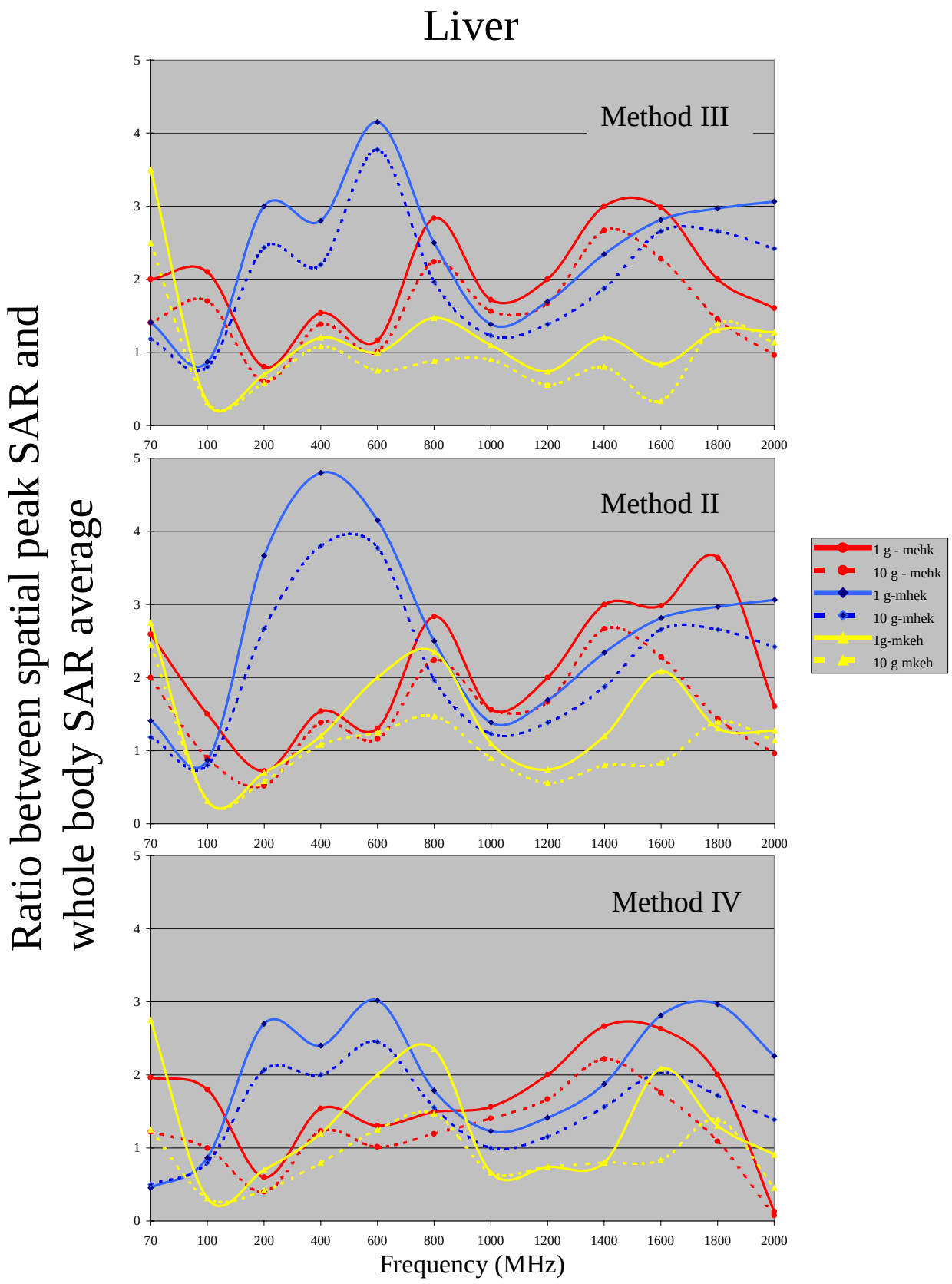

Figure 20. Ratios between peak localized SAR and whole body SAR average for lung outer for various mass intervals (1g and 10 g), orientations (MEHK; MHEK, MKEH) and frequencies (70-2000 MHz) by considering three different methods (algorithm).

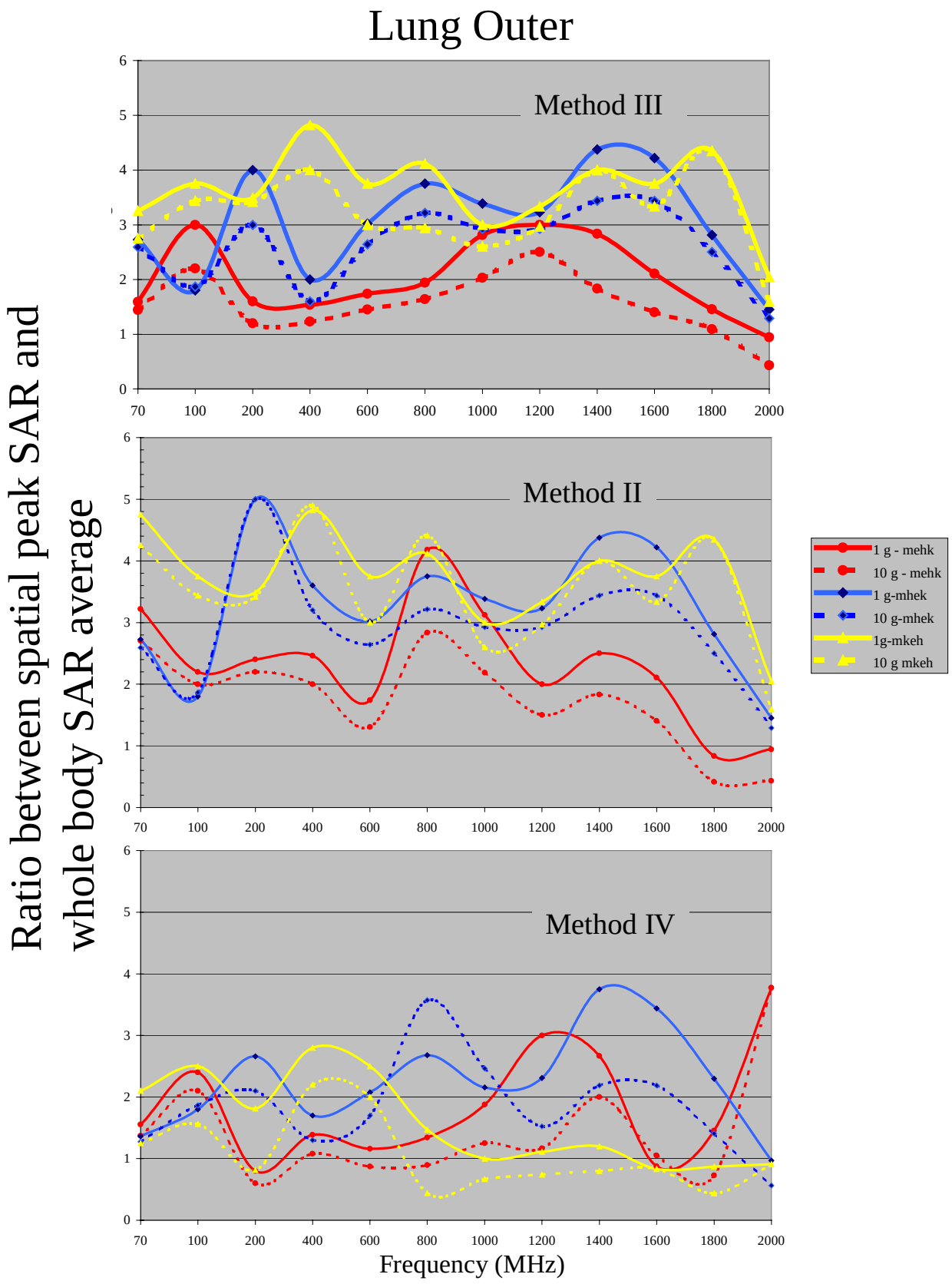

Figure 21. Ratios between peak localized SAR and whole body SAR average for lung inner for various mass intervals (1g and 10 g), orientations (MEHK; MHEK, MKEH) and frequencies (70-2000 MHz) by considering three different methods (algorithm).

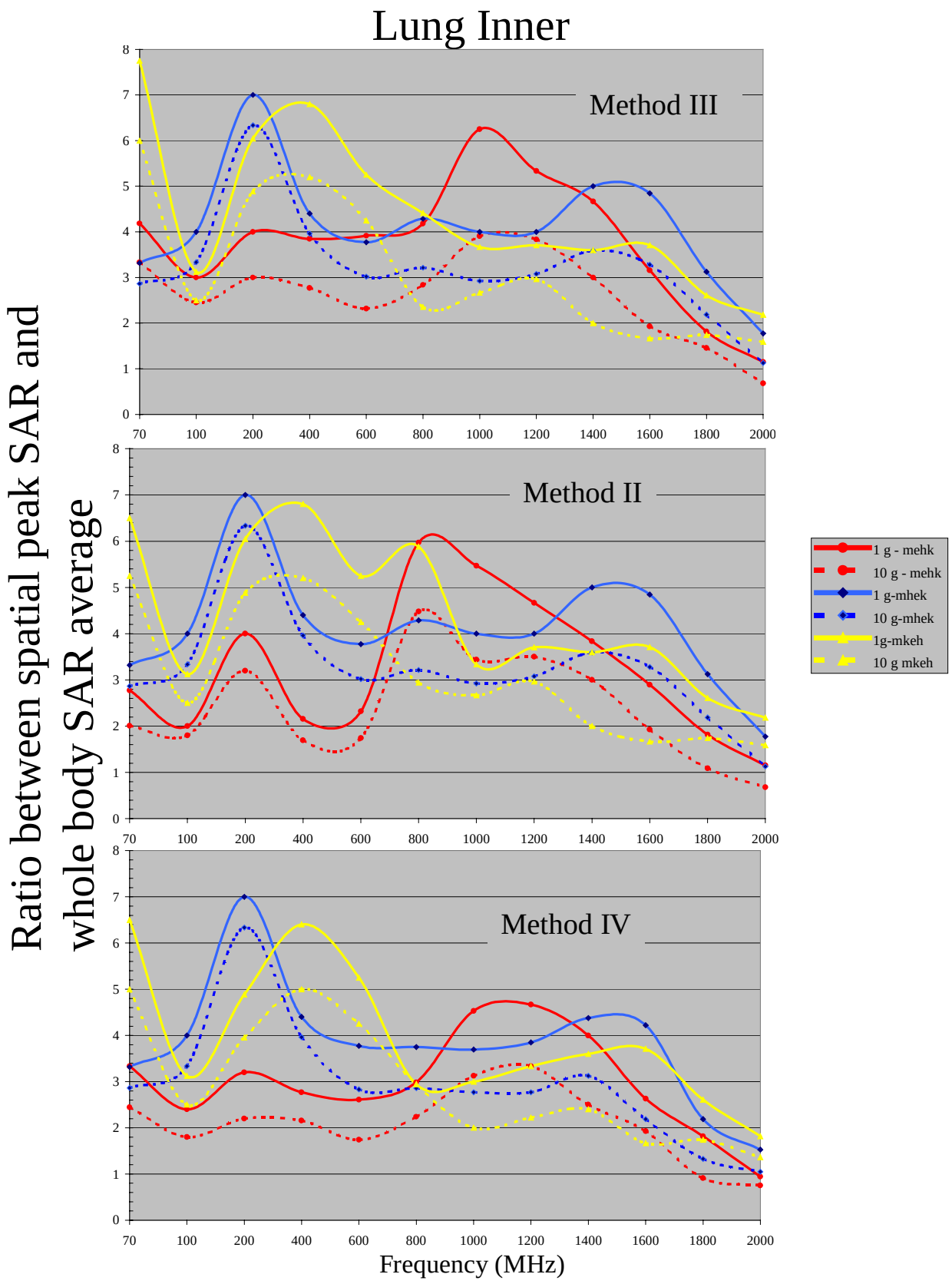

8. DISCUSSION

This research examined the extent to which differences in voxel sizes of the anatomical man models influence whole body SAR average values and spatial peak SAR values averaged over 1 g and 10 g of tissue. This work contributes to understanding the mechanisms of interaction of RF fields with biological systems and to the SAR dependence on various averaging volumes, thus leading to increased understanding of the validity of numerical calculations.

Inter-comparison of the data clearly demonstrated that voxel size had minor impact on the predicted whole body SAR values. Despite differences between individual organ mass in all applied anatomical man models (voxel sizes: 3, 10 and 22 mm^3) and modified anatomical structure, whole body SAR average remains within $\pm$ 20%. The only limitation represents the voxel size of the used model versus frequency of interest.

In contrast to whole body SAR predictions, the voxel size as well as averaging mass interval had substantial influence on spatial peak SAR calculations. The present work showed that detailed anatomical structure (smaller voxel size) of the used digital models converge to lower absolute SAR values and, thus, to lower ratios between spatial peak and whole body SAR. On the other hand, relatively high ratios between spatial peak SAR and whole body averaged SAR obtained by coarser anatomical models (10 and 22 mm^3) are very unlikely in real exposure situations of the human. When the voxel size increases small organs may be distorted or lost, some symmetries may be affected, organs will change mass slightly and the continuity of elongated structures may be disrupted. Therefore, spatial peak SAR values obtained by coarser anatomical models were higher for at least factor of 1.3. In some investigated situations, the differences exceeded even factor of 4. From one point of view, such overpredictions (worst case conditions) could be acceptable when quick and superficial estimations are required and, at the same time, the accuracy of the results is not crucial. On the other hand, more detailed and precise predictions of localized SAR values would be desirable particularly in relation with near field exposure condition where only limited area of the target tissues or organs might be affected. As stated above, spatial peak SAR values are dramatically dependent on the size of the voxels. Thus, the use of high resolution models with detailed anatomical structure for spatial peak SAR predictions is highly recommended.

A comprehensive parametric analysis of the ratios between spatial peak SAR and whole body SAR average demonstrated significantly elevated peak SAR value (up to 53.3 at MEHK, 47.8 at MKEH and 73.3 at MHEK) in a finest resolution (3mm^3) man model. These ratios are substantially greater than 20-times the whole-body average SAR introduced in health and safety standards. With some exceptions, the spatial peak SAR was mainly found in the ankle region for muscle tissue type. It is interesting to note that while specifications on local SAR were first included in the IEEE standard as early as 1982, even earlier laboratory work had already demonstrated the possibility of significantly higher spatial peak SAR from the ratio of 20 [Guy et al. 1976]. This finding has played a significant role in deriving limits for peak SARs; for example, the present

assumption of a 20 to 1 ratio between local peak and whole-body average SARs dictates the local limit for exposures of all kinds, regardless of whether the exposure occurs in the far field or the near field.

It should be stated that only far field exposure conditions were considered in our study. For near field exposure, varying the ration between electric and magnetic field might lead to different results. Therefore, near-field exposures should be compared with far-field exposures for the same peak incident power density relative to spatial peak and whole-body average SARs. However, it would appear desirable to reevaluate the local SAR enhancement factor found in the body of both experimental research animals as well as humans when exposed to non-uniform fields.

One of the objectives of this project was to analyze different algorithms for determination of the peak spatial SAR averaged over certain mass (1g or 10 g) in individual tissue/organ. We have developed three different procedures (methods II, III and IV) for calculating spatial peak SAR in individual tissue or organ. It was demonstrated that spatial peak SAR values are substantially dependent also on the algorithm (method) used in averaging procedures. Inter-comparison between all different methods showed that an uncertainty between 1.2 and 2.0 exists for different exposure conditions. The method IV that searches for the cube containing the required mass with the smallest extension (smallest number of the corresponding voxels of the chosen tissue/organ) was chosen as the basis for the evaluation of the spatial peak SAR. This particular method seems to be the most appropriate for calculating the peak spatial SAR averaged throughout the entire individual tissue/organ by optimizing the selected area for searching the voxels with the highest SAR values.

In addition, special emphasis on spatial peak SAR averaged over 1 g or 10 g of target tissues including critical survival organs was made. We found that muscle is the primary site of interaction of electromagnetic energy and, thus, the highest absolute SARs as well as relative ratios between spatial peak and whole body SAR average were reported (up to factor of 50). Preliminary results [Mason et al. 2000, Gajšek et al. 2001] obtained from using FDTD code to predict localized SAR values in various tissues have revealed that high water content tissues including muscle absorb more energy from RF fields than less wet tissues and are, thus, more lossy. Since muscle is spread through the whole human body, it forms complex multiple tissue layers and affects the localized SAR values in the majority of the surrounding tissues and organs. Since the highest ratios were observed for skin, fat and muscle in all applied combinations of orientations and frequencies, these findings indicate that selected central organs are reasonably well shielded by these tissues, in particular the muscle where the greatest portion of the incident energy has been absorbed.

The present work showed that spinal cord and cerebral spinal fluid could be listed among the tissues with medium absorption coefficient since the ratios between spatial peak and whole body SAR were lower than factor of 30 for all applied combinations of orientations and frequencies.

However, several investigators [Wang et al. 1999, Gandhi 2000] have previously reported that due to great heterogeneity of the human model, possible effects related to RF fields may be organ dependent. The

brain (white and gray matter) is considered to be the most interested target tissue because of its critical control function. Most research projects worldwide are related to the brain, such as DNA damage in brain cells and brain cancer risk. A detailed analysis of the localized peak SARs in relation to the whole body SAR for various exposure conditions in the brain demonstrated that the ratios never exceeded the factor of 15. For the white and gray matter, the localized resonance was found around 900 MHz at MKEH orientation whereas at other two orientations lower ratios with no substantial resonance were reported. As mentioned earlier, localized SARs could be changed dramatically when near field exposure occurred. Gandhi et al. [1999] reported that in some near-field exposure situations, e.g., hand-held cellular telephones, the peak SAR values were generally observed at or near the surface of the ear, which is irregular in shape and is made up of skin, fat and cartilage with skull bone and brain behind this region.

The ratios between spatial peak and whole body SAR in other central organs under investigation (inner and outer lung, liver, heart) were lower than factor of 10 and, thus, the localized absorption of incident RF energy was close to the whole body SAR average.

The SAR, which is proportional to the tissue heating (thermal effects), represents the basic restriction of exposure to RF fields in health and safety standards. Although there is considerable experimental literature on whole body effects to support standard setting activities, standards for localized exposure have been based on models and extrapolations that leave unclear the biophysical basis for limiting energy input into a localized tissue volume. In order to protect against too great increase in temperature in small region of the body, it is necessary to define appropriate volume for determining spatial peak SAR average. As mentioned earlier, two concepts (1g and 10 g) on averaging volume are being currently used in standards. Present research indicates that SARs averaged over 1 g of tissue could be as much as two times higher than those obtained by 10 g averaging procedure. This was demonstrated for almost any combination between individual tissue, its orientation and frequency.

The ratio between spatial peak SAR averaged over 1 g of tissue and whole-body SAR values substantially exceeded the ratio of 20 currently introduced in standards. While this was clearly demonstrated for some tissues (muscle, fat, skin) over wide range of frequencies and different orientations much lower ratios were established for some critical survival organs (white and gray matter, heart, liver, inner and outer lung, nerve spinal). The ratios between spatial peak SAR averaged over 10 g of tissue and whole-body SAR values for all selected tissues were close to factor of 20. However, it could be stated that 20 to 1 ratio between spatial peak and whole-body average SARs is somehow reliable with present data but should be further discussed particularly in connection with averaging volume (1g or 10 g). The question which averaging volume should be used as a basis for the test compliance still seems to be scientifically unsolved issue and the possible solutions are rather politically motivated.

Electromagnetic fields standards and compliance to the standards are based, in part, on experimental data and the replication of these data. Therefore, accurate RF dosimetry is an essential component in

designing, replicating, or confirming an experiment. To ensure compliance with safety guidelines during equipment design, manufacturing and maintenance, realistic and accurate models could be used as a bridge between empirical data and actual exposure conditions. Before these tools are transitioned into the hands of health safety officers and designers, their sensitivity, accuracy, and limitations must be known in relation to the variability in different models' parameters including exposure conditions. Accurate predictions of localized and whole-body SAR values by computer models may lead to minimizing the safety margin and, therefore, to modification of existing safety standards. Furthermore, higher quality dosimetry will lead to more precise data that are critical in the harmonization of the EMF standards.

It is hoped that the global harmonization of the health and safety standards will benefit from ongoing research in the field of RF dosimetry. Thus, the next generation of standards would be able to incorporate the latest information on dosimetric data including health risks within the same harmonized standards framework.

.

9. REFERENCES

Caputa K, Okoniewski M, Stuchlz MA, An Algorithm for computation of the power deposition in human tissue, IEEE Antennas and propagation Magazine, Vol 41, No 4., 1999

EN (European Standard) 50360, Product standard to demonstrate the compliance of mobile telephones with the basic restrictions related to human exposure to electromagnetic fields, CENELEC, Brusseles, 2001

Chou CK, Bassen H, Osepchuck J, Balzano Q, Peterson R, Meltz M, Cleveland R, Lin JC, and Heynick L Radio frequency electromagnetic exposure: Tutorial review on experimental dosimetry, Bioelectromagnetics 17, 341-353. 1996

Durney CH, Johnson CC, Barber PW, Massoudi H, Iskander MF, Lords JL, Ryser DK, Allen SJ, Mitchell JC Radiofrequency radiation dosimetry handbook. SAM-TR-78-22, Brooks Air Force Base, San Antonio, TX, 1986

Gabriel C. Compilation of the Dielectric Properties of Body Tissue at RF and Microwave Frequencies, Brooks AFB, TX: Armstrong Laboratory Report, AL/OE-TR-1996-0037, 1996

Gajšek P, Hurt WD, Ziriax JM, Mason PA. Parametric dependence of SAR on permittivity values in a man model. IEEE trans. biomed. eng., Vol. 48, No. 10, pp 1169-1177, 2001

Gandhi OP, Numerical and experimental methods for dosimetry of RF radiation – some recent results, In Klauenberg BJ and Miklavčič D, (eds.) "Radio Frequency Radiation Dosimetry and Its Relationship to the Biological Effects of Electromagnetic Fields." Kluwer Academic Publishers B.V., Dordrecht, The Netherlands, 112-121, 2000

Gandhi OP, Lazzi G, Tinniswood A, and Yu Q, Comparison of numerical and experimental Methods for determination of SAR and Radiation patterns of Handheld Wireless Telephones, Bioelectromagnetics, No. 20, 93-101, 1999

Guy, A. W., Webb, M. D., and Sorensen, C. C., Determination of power absorption in man exposed to high frequency electromagnetic fields by thermographic measurements on scale models, IEEE Transactions on Biomedical Engineering BME-23, 361-370, 1976

Hurt WD, Absorption characteristics and measurement concepts, In Klauenberg BJ and Miklavčič D, (eds.) "Radio Frequency Radiation Dosimetry and Its Relationship to the Biological Effects of Electromagnetic Fields." Kluwer Academic Publishers B.V., Dordrecht, The Netherlands, 39-52., 2000

ICNIRP - International Commission of Non-ionizing Radiation Protection, Guidelines for Limiting Exposure to Time-Varying Electric, Magnetic, and Electromagnetic fields (up to 300 GHz), Health Phys. 74, 494 – 522; 1998

IEEE - Institute of Electrical and Electronics Engineers, Inc. Standard for Safety Levels with Respect to Human Exposure to Radio Frequency Electromagnetic Fields, 3 kHz to 300 GHz, Institute of Electrical and Electronics Engineers, New York, 1999

IEEE- Institute of Electrical and Electronics Engineers, Inc., C95.3-1991 Revision Draft CBD-1, Draft recommended practice for measurements and computations with respect to human exposure to RF electromagnetic fields, 100 kHz to 300 GHz, 2001

Kunz KS and Lee KM. A three-dimensional finite-difference solution of the external response of an aircraft to a complex transient EM environment, 1. The method and it's implementation. IEEE Transactions on Electromagnetic Compatibility, Vol. 20, p. 328, 1978

Kunz KS and Luebbers RJ. “The Finite Difference Time Doman Method for Electromagnetics”, CRC Press, Inc., Boca Raton, FL, 1993.

Lin JC, Perspectives on guidelines for human exposure to RF radiation, IEEE Antennas and Propagation Magazine, 42(1), 147-148., 2000

Mason PA, Hurt WD, Walters TJ, D’Andrea JA, Gajšek P, Ryan KL, Nelson PA, and Ziriax JA: Effects of frequency, permittivity, and voxel size on predicted specific absorption rate values in biological tissue during electromagnetic field exposure, IEEE Microw. Theory & Techn, Vol.48, No 11, 2050-2057, 2000.

Mason PM, Walters TJ, Fanton JW, Erwin DN, Gao JH, Roby JW, Lott KA, Lott LE, Blystone RV. Database created from magnetic resonance images of a Sprague-Dawley rat, rhesus monkey, and pigmy goat. FASEB J., 9:434-440, 1995

Mason PM, Ziriax JM, Hurt WD, D’Andrea JW. 3-Dimensional models for EMF dosimetry. In Electricity and Magnetism in Biology and Medicine edited by Bersani, Kluwer Academic/Plenum Publishers, 1999

Sheppard AR: Thermal basis for the averaging volume for RF safety standards, Workshop, RF fields applied in wireless communication – biological effects and safety concerns, Bioelectromagnetic society, 2000

Taflove A and Brodwin ME, Computation of the electromagnetic fields and induced temperatures within a model of the microwave irradiated human eye, IEEE Transactions on Microwave Theory and Techniques, MTT-23, 888, 1975

Wang J, Joukuro T, Fujiwara O, Uncertainty of the One –Gram Averaged spatial peak SAR in human head for portable telephones due to average procedures, T.IEE Japan, Vol. 119_c, No. 1, 1999